

**UNIVERSITY OF GAZİANTEP
GRADUATE SCHOOL OF
NATURAL & APPLIED SCIENCES**

FINITE ELEMENT ANALYSIS OF ENCLOSED DIE

**FORGING OF
AXISYMMETRIC PARTS**

M. Sc. THESIS

IN

MECHANICAL ENGINEERING

BY

ÖMER YETKİN

MAY 2017

MAY 2017

M.Sc. in Mechanical Engineering

ÖMER YETKİN

Finite Element Analysis of Enclosed Die Forging of Axisymmetric Parts

M.Sc. Thesis

in

Mechanical Engineering

University of Gaziantep

Supervisor

Prof. Dr. Ömer EYERCİOĞLU

by

Ömer YETKİN

May 2017



© 2017 [Ömer YETKİN]

REPUBLIC OF TURKEY
UNIVERSITY OF GAZİANTEP
GRADUATE SCHOOL OF NATURAL & APPLIED SCIENCES
MECHANICAL ENGINEERING

Name of the thesis: Finite Element Analysis of Enclosed Die Forging of
Axisymmetric Parts

Name of the student: Ömer YETKİN

Exam date: 15.05.2017

Approval of the Graduate School of Natural and Applied Sciences


Prof. Dr. A. Necmeddin YAZICI

Director

I certify that this thesis satisfies all the requirements as a thesis for the degree of
Master of Science.


Prof. Dr. Sait SOYLEMEZ

Head of Department

This is to certify that we have read this thesis and that in our consensus/majority
opinion it is fully adequate, in scope and quality, as a thesis for the degree of Master
of Science.


Prof. Dr. Ömer EYERCİOĞLU

Supervisor

Examining Committee Members

Prof. Dr. İ. Hüseyin FİLİZ

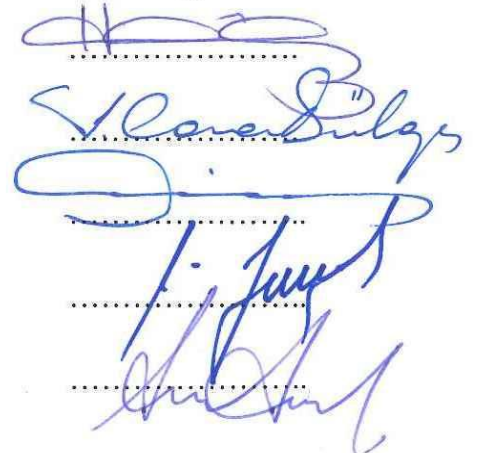
Prof. Dr. L. Canan DÜLGER

Prof. Dr. Ömer EYERCİOĞLU

Assoc. Prof. Dr. Necip F. YILMAZ

Assist. Prof. Dr. Mustafa DÜLGER

Signature



I hereby declare that all information in this document has been obtained and presented in accordance with academic rules and ethical conduct. I also declare that, as required by these rules and conduct, I have fully cited and referenced all material and results that are not original to this work.

Ömer YETKİN

ABSTRACT
FINITE ELEMENT ANALYSIS OF ENCLOSED DIE FORGING
OF AXISYMMETRIC PARTS

YETKİN, ÖMER
M.Sc. in Mechanical Engineering Department
Supervisor: Prof. Dr. Ömer EYERCİOĞLU
May 2017
53 pages

In this thesis, the finite element analysis of enclosed die forging of axisymmetric parts is studied. Prediction of the exact behavior of enclosed die forging process is becoming increasingly essential and it also important to optimize the process design to reduce the required load and consumed energy. In this study, evaluation of forging load and metal flow for H-shape part by using various punch/counter-punch movements and various preforms are presented. By using a finite element analysis (FEA), uni-directional forging and bi-directional loading conditions for two types of preforms (upset and extrusion mode of deformation) are compared in terms of forging load, deformation energy and metal flow under different friction conditions. The effects of rib angle and hub thickness of H-shape forgings on the forging load and energy are also shown. The experimental work is carried out by using a modeling material (plasticine) for verification. The results show that the forging load asymptotically increases at the final stage of the forging where the corner filling of the die cavity. The maximum forging load is considerably reduced by using the bi-directional step loading (divided flow), therefore, the usage of servo-driven presses are very effective. The material flow in bi-directional forging of the H-shape is symmetrical while the flow in uni-directional forging is non-symmetrical. The non-uniform material flow increasing the deformation resistance and friction load.

Key Words: FEM, enclosed die forging, divided flow, bi-directional loading

ÖZET

EKSENEL SİMETRİK PARÇALARIN TAM KAPALI KALIPTA DÖVME İŞLEMİNİN SONLU ELEMANLAR YÖNTEMİYLE ANALİZİ

YETKİN, ÖMER

**Yüksek Lisans Tezi, Makine Müh. Bölümü
Tez Yöneticisi: Prof. Dr. Ömer EYERCİOĞLU**

Mayıs 2017

53 sayfa

Tez çalışmasında eksenel simetrik parçaların tam kapalı kalıpta dövme işleminin sonlu elemanlar yöntemiyle analizi yapılmıştır. Tam kapalı kalıp dövme işleminin kesin davranışının tahmini giderek önem kazanmaktadır ve gerekli yükü ve tüketilen enerjiyi azaltmak için proses tasarımını optimize de önemlidir. Bu çalışmada, H-şekilli parça için dövme yükü ve metal akışının çeşitli zımba/karşı zımba hareketleri ve çeşitli önşekiller kullanılarak değerlendirilmesi sunulmuştur. Sonlu elemanlar analizi (FEA) kullanılarak, iki tip önşekil için farklı sürtünme koşullarında, tek yönlü ve iki yönlü dövme koşulları (basma ve ekstrüzyon şekil değiştirme modu); dövme yükü, şekil değiştirme enerjisi ve metal akışı açısından karşılaştırılmıştır. Dövme yükü ve enerjisi üzerindeki; yanak açısının ve göbek kalınlığının H-şekilli parça üzerindeki etkileri de gösterilmiştir. Deneysel çalışma, doğrulama için bir modelleme malzemesi (oyun hamuru) kullanılarak gerçekleştirilmiştir. Sonuçlar, kalıp köşe boşluğunun doldurulmasının gerçekleştiği dövmenin son aşamasında dövme yükünün asimptotik olarak arttığını göstermektedir. Maksimum dövme yükü, iki yönlü-iki aşamalı basma (bölünmüş akış) kullanılarak önemli ölçüde azaltılmıştır, bu nedenle servo tahrikli preslerin kullanımı çok etkilidir. H-şeklinin iki yönlü dövülmesindeki malzeme akışı simetrik iken, tek yönlü dövme de malzeme akışı simetrik değildir. Düzgün olmayan malzeme akışı şekil değiştirme direncini ve sürtünme yükünü artırır.

Anahtar Kelimeler: SEM, kapalı kalıpta dövme, bölünmüş akış, iki yönlü basma



To My Family

ACKNOWLEDGEMENTS

I would like to express my sincere gratitude to my supervisor, Prof. Dr. Ömer EYERCİOĞLU for encouragement, guidance, suggestion and help in making this thesis understandable.

I am very thankful to my parents, mom and dad for their patience for long time of my life.

I am thankful to my family, my wife and two sons.

I am thankful to my friends.

Finally, I am very thankful to my master, Prof. Dr. Haydar BAŞ for his directionism, leadership and fatherliness.

CONTENTS

	Page
ABSTRACT	v
ÖZET.....	vi
ACKNOWLEDGEMENT	viii
CONTENTS	ix
LIST OF TABLES	xi
LIST OF FIGURES	xii
LIST OF SYMBOLS	xv
CHAPTER 1	1
INTRODUCTION	1
1.1 Introduction	1
1.2 Thesis Layout	2
CHAPTER 2	3
LITERATURE SURVEY	3
2.1 Enclosed Die Forging and Utilization of Servo Press	3
2.2 Finite Element Analysis of Precision Forging.....	5
2.3 The Contribution of Study	6
CHAPTER 3	7
ENCLOSED DIE FORGING AND FINITE ELEMENT METHOD	7
3.1 Enclosed Die Forging	7
3.2 Presses for Enclosed Die Forging.....	10
3.3 Finite Element Method	11
CHAPTER 4	15
FE MODELLING AND EXPERIMENTAL STUDY.....	15
4.1 Fe Modelling	15
4.1.1 H-Shaped Part Geometry	16
4.1.2 Preform Geometry	17
4.1.3 The Loading Conditions	18
4.1.4 Preform Material.....	19
4.2 Experimental Study	19

4.2.1 Modeling Material and Plasticine Specimen Preparation	19
4.2.2 Compression Test	20
4.2.3 Forging Press and Die Set.....	20
4.2.4 H-Shape Forging of Plasticine.....	21
CHAPTER 5	22
RESULTS AND DISCUSSION	22
5.1 Experimental Results.....	22
5.1.1 Compression Test and Flow Curve of Plasticine	22
5.1.2 H-Shape Forging of Plasticine.....	23
5.2 FE Results.....	23
5.2.1 Plasticine Simulations.....	23
5.2.2 Aluminum 1100 Forgings.....	25
5.2.2.1 Effect of Loading Direction on Forging Load and Energy of Preform (P1) Upset Mode	26
5.2.2.2 Effect of Loading Direction on Forging Load and Energy of Preform (P2) Extrusion Mode	32
5.2.2.3 Dividing Metal Flow by Using Bi-Directional Step Forging Load ...	36
5.2.2.4 Quality of Forged Product in Terms of Metal Flow.....	39
5.2.2.5 Effect of Rib Angle (α) on Forging Load.....	42
5.2.2.6 Effect of Hub Thickness (t) on Forging Load and Energy.....	47
CHAPTER 6	48
CONCLUSION AND FUTURE WORK	48
6.1 Conclusions	48
6.2 Future Work	49
REFERENCES.....	50

LIST OF TABLES

	Page
Table 4.1 Dimensions of variables of Preforms and H-Shaped Forgings	16
Table 5.1 Al 1100 Forging Load Results of Simulations	25
Table 5.2 Al 1100 Energy Consumption Results of Simulations.....	26
Table 5.3 The maximum Uni-directional and Bi-directional forging loads for various friction factor (m)	30
Table 5.4 The maximum loads for uni-directional, bi-directional and bi-directional step	39
Table 5.5 The max. forging loads for uni-directional, bi-directional and bi-directional step	43

LIST OF FIGURES

	Page
Figure 3.1 Enclosed-die forging. 1) billet; 2) upper die; 3) lower die; 4) upper punch; 5) lower punch; 1) finished part	8
Figure 3.2 Comparison of a) classical semi-closed die forging and b) enclosed die forging of cross pin	9
Figure 3.3 Enclosed die forging methods and products. a-One moving punch, b-Two moving punches	9
Figure 3.4 Multi-action press	10
Figure 3.5 Sectional view of the drive mechanism of the Aida Digital Servo Former	11
Figure 3.6 Some example settings of forming motions and speeds	11
Figure 3.7 The elements and nodes formed by the process of discretization	13
Figure 4.1 Geometric Model of H-Shaped (a) Preform (b) Forged product	15
Figure 4.2 Geometric Model of Forged H-Shaped Products	16
Figure 4.3 Geometric Model of Preforms for H-Shape Forging	17
Figure 4.4 a) Preform P1 $d_i=17$ mm upset mode of metal flow b) Preform P2 $d_i=10$ mm extrusion mode of metal flow	17
Figure 4.5 FE Model of H-Shaped upset mode forging (P1) of initial and final step of three loading conditions; a) uni-directional, b) bi-directional c)bi-directional step	18
Figure 4.6 FE Model of H-Shaped extrusion mode forging (P2) of initial and final step of three loading conditions; a) uni-directional, b) bi-directional c)bi-directional step.....	19
Figure 4.7 The material data of Aluminum 1100 taken form DEFORM Database ..	19
Figure 4.8 Photograph of the servo-press used in forging experiment	21
Figure 4.9 Sketch of the die set	21
Figure 5.1 The load-stroke diagram of the plasticine specimens in the compression test	22

Figure 5.2 The flow stress curve of the plasticine	22
Figure 5.3 Experimental and FE load-stroke diagram of H-Shape plasticine forgings	23
Figure 5.4 The FE output of plasticine H-shape forgings a) Uni-directional b) Bi-directional loading	24
Figure 5.5 Forging load-stroke diagram and equivalent stress distribution of Aluminum 1100 H1-P1 for a) uni-directional forging and b) bi-directional forging	27
Figure 5.6 Forging energies of H-shape Aluminum 1100 forgings H1-P1 for a) uni-directional and b) bi-directional loading	28
Figure 5.7 Uni-directional and Bi-directional forging loads for H1P1 with different friction factors (m).....	29
Figure 5.8 Upset mode of the material flow pattern of H1-P1 -shape Aluminum 1100 b) bi-directional loading	31
Figure 5.9 Forging load-stroke diagram and equivalent stress distribution of Aluminum 1100 H1-P2 for a) uni-directional forging and b) bi-directional forging	32
Figure 5.10 Forging energies Aluminum 1100 forgings H1-P2 for a) uni-directional and b) bi-directional loading	33
Figure 5.11 Uni-directional and Bi-directional forging loads with different friction factors for H1P2-shape (m=0 and m=0.4).....	34
Figure 5.12 Extrusion mode of the material flow pattern of H1-P2 Aluminum 1100 with friction factor (m=0.4) forgings for a) uni-directional and b) bi-directional loading	35
Figure 5.13 Sketch of Divided Flow Die Set for bi-directional step loading	36
Figure 5.14 The FE output of H1P1-shape forgings Bi-directional step loading	37
Figure 5.15 The FE output of H1P2-shape forgings Bi-directional step loading	37
Figure 5.16 Uni-directional, bi-directional and bi-directional Step forging loads for H1P1 and H1P2 (m=0.4)	38
Figure 5.17 Flownet of H1P1-shape (m=0.4) for a)Uni-Directional b)Bi-Directional c) Bi-directional step	40
Figure 5.18 Flownet of H1P2-shape (m=0.4) for a)Uni-Directional	

b)Bi-Directional c) Bi-directional step	41
Figure 5.19 Effect of Rib Angle on the Forging Load	42
Figure 5.20 Flow net of H4P1 (m=0.4) for a)uni-directional b)bi-directional c) bi-directional step.....	44
Figure 5.21 Flownet of H4P2(m=0.4) for a)uni-directional b) bi-directional c) bi-directional step.....	45
Figure 5.22 The velocity distrubution of bi-directional forgings with friction factor (m=0.4) for a) H4P1 upset mode b) H4P2 extrusion mode	46
Figure 5.23 Uni-Directional and Bi-Directional Forging Loads according to hub thickness (t) for Preform P1 and P2 for H1, H9 and H12 parts	47
Figure 5.24 The change in forging energies with respect to hub thichness	47

LIST OF SYMBOLS/ABBREVIATIONS

H	The final height of H-Shape Part
D_h	The hub diameter of H-Shape Part
D_o	The outer diameter of H-Shape Part
D_i	The inner diameter of H-Shape Part
t	The hub thickness of H-Shape Part
α	The rib angle of H-Shape Part
h	The heights of preform
d_i	The inner diameter of preform
d_o	The outer diameter of preform
P1	Preform with upset mode of deformation
P2	Preform with extrusion mode of deformation
m	Friction factor
σ	Engineering stress
ε	Engineering strain
σ_t	True stress
ε_t	True strain

CHAPTER 1

INTRODUCTION

1.1 Introduction

Enclosed die forging is one of the precision forging processes. In this process, the billet is located in the die cavity and is squeezed by one or more rams. As compared with the conventional flashless die forging, in which the billet is compressed between the upper and lower dies, the die cavity can be filled under a lower forming load owing to the reduction of the contact area between the loading punch and the billet material. But as the billet material fills the die cavity, the forming pressure increases sharply. Therefore, it is very important to reduce the forming pressure at the final stage of the process [1, 2].

Net shape forging with enclosed die forging technology which has come into practical use recently has large potentiality. It has been applied in cold and warm forging fields. Application to semi-hot forging with simplified enclosed forging die-sets is also increasing. The products by enclosed die forging are becoming larger. Application to general industries other than automotive ones is increasing as well [3].

With recent advancements in software development and the availability of more powerful computers, a finite element analysis (FEA) package called DEFORM has enabled this entire forging process to be simulated, while simultaneously predicting all the necessary stress–strain states in both die and workpiece [4].

Recently, there has been a growing demand for developing enclosed die forging using the servo-press for the forging industry across the world. The development of servo-press realizes the complex and flexible press motion [5-8].

Moreover, forging load, deformation energy and material flow pattern is more complicated and difficult to predict in enclosed die forging. Prediction of the exact behavior of enclosed die forging process is becoming increasingly essential and it also important to optimize the process design to reduce the required load and consumed

energy. Finite element analyses (FEA) have been greatly successful to provide the understanding of metal flow and die stresses for different forming processes, especially a precision forging process of enclosed die forging.

In this thesis, the finite element analysis of enclosed die forging of axisymmetric parts is studied. The evaluation of forging load and metal flow for H-shape part by using various punch/counter-punch movements and various preforms are presented. By using a finite element analysis (FEA) package (DEFORM™); uni-directional forging, bi-directional loading and bi-directional step loading conditions for two types of preforms (upset and extrusion mode of deformation) are compared in terms of forging load, deformation energy and metal flow under different friction conditions.

1.2 Thesis Layout

This thesis organized in six chapters.

The following chapter, chapter 2, expresses the most related works and studies on enclosed die forging, servo presses on forming process and finite element analyses of precision forging processes.

In chapter 3, the general theory of enclosed die forging, using presses on forming processes and Finite Element Method (FEM) of metal forming are presented.

In chapter 4, the FEM based DEFORM 2D™ commercial software package was used to attain all FE modeling, part geometries, preform geometries, loading simulation models belong to load, energy and metal flow analysis of enclosed die forging operations. Experimental procedure and servo press used in experimental work are also given in this chapter.

In chapter 5, the experimental and FE results are presented. Comparison of plasticine and Al 1100 forging load FE results of 14 H-Shape parts are presented. These are with various frictions, shapes, loading directions (uni-directional, bi-directional and bi directional step) and 2 various preforms (using on upset and extrusion mode) are presented for 14 H-Shaped part.

Conclusion and recommendations for future works are also provided in chapter 6.

CHAPTER 2

LITERATURE SURVEY

In the literature, there are many studies available on the investigation of enclosed die forgings, finite element analyses and application of servo presses. While there have been many studies, the summary of some of the mostly related ones on the subject of the thesis are summarized.

2.1 Enclosed die forging and utilization of servo press

Yoshimura et al. [9] investigated the net shape forming method of enclosed die forging technology which had come into practical use. By controlling the motion of upper and lower punches, the optimum condition of enclosed die forging could be obtained near-net shape products with high precision in low costs.

Osakada et al. [10] proposed a method employing an axially driven container in order to reduce the forming pressure of precision forging to a feasible level. By this method for enclosed-die forging when the billet was squeezed by the punch, the container was moved in one cycle or oscillation, then the material flow speed could be under control and forming pressure was decreased significantly.

Shi et al. [11] studied near net shape forming process of titanium alloy impeller. 3D FEM model was simulated and experimental studies were carried out in the study. Billet shape, die structure and loading scheme were studied and the parts were forged by using isothermal enclosed die forging technology for controlling the metal flow and improving the forgeability.

Shan et al. [12] described the process of precision forging of an aluminum-alloy rotor with 23 radial blades which has very complex shape. In order to reduce forging pressure or to improve the die fill, a lot of forming methods were employed. The difficulty was filling very end of the blades completely. They suggested that isothermal fully-enclosed die forging could precisely produce the rotor, it reduces

the machining time and the processing cost by improving mechanical properties of the forging.

Gronostajski et al. [13] concerned with the development of precision forging about its quality, tool shape, lubrication, cooling, process speed, press settings, slug geometry and preform temperature. They showed that the advantages of precision forging over other technologies in terms of material savings and quality.

Behrens et al. [14] presented precision forging processes for high-duty automotive components, such as helical gears and crankshafts. They were suggested multi-stage forging including preforming operations for the success of the process.

Xue et al. [15] worked on the process of isothermal precision forging of a cylindrical aluminum-alloy housing which is a key part of Z11 helicopter. It was expressed that the lubricant, residual stress, die chilling and the application of forging load were the main factors that affect the process.

Shan et al. [16] described the problems of complex-shaped light alloy components in precision forging. Improving the die fillings and reducing the forging loads, they were used a method in which plastic mats exerting die-locking pressure and a female die adopted.

Chi et al. [17] presented a new multi-row sprocket tooth profile with simulating the semi-precision forging. In order to fully fill the die cavity, axial, radial and circumferential velocity directions and curves were set and compared.

Guan et al. [18] proposed a multi-step die forging to optimize preform shape. They applied this new approach for complex parts of forging process of the pendulum mass forging and tried to optimize forging with no defects and with a small amount of flash.

Kawamoto et al. [19] used back-pressure to improve shape accuracy and to reduce the total forming load during cold forging. A servo die cushion was used for the forging process. They suggested that back-pressure application was a proper method to reduce forming load and to minimize the unfilled area.

Kim et al. [20] investigated the effect of forming speed in precision forging process. They have used a high-performance servo press and additional three hydraulic servo

driven die cushions to facilitate four axes motion control. They were forged a spur gear to show the effect of press motion on forging load and die filling.

2.2 Finite Element Analysis of Precision Forging

According to Altan et al. [21] the global competition requires that the forging industry utilize practical and proven computer aided engineering (CAE) technologies for rapid and cost effective process design, to analyze and optimize the metal flow and conduct die stress analyses before forging trials. The numerical simulation of forging process with finite element method (FEM) based codes assisted the forging engineer in establishing and optimizing process variables and die design.

MacCormack et al. [22] performed finite element analyses (FEA) by using DEFORM software package. The forging operations were modeled using 2D finite element analysis (FEA) because of the symmetry of a complex part. They used the Flow Net pattern within DEFORM to observe material flow pattern during entire process.

Petrov et al. [23] studied the development of isothermal enclosed die forging technology of an axisymmetric aluminum part with flange. The optimum conditions of forging were obtained by means of FEM simulation. Experimental work was carried out and FEM simulation results were compared with the experiments. They concluded that the forging process design by using FEM simulation was to ensure adequate metal flow in the dies so that the desired finished part geometry could be obtained without defects and with advanced mechanical properties.

Uğur, T.[24] investigated the metal flow of axisymmetric; U-Shape, T-Shape and H-Shape parts in net-shape forging process to obtain the optimum preform geometry. The forged part geometries were evaluated to reducing the forging load and energy by using the FEM simulations and experimental studies. It was expressed in the thesis that extrusion mode preforms requires lower loads than the upsetting mode preforms.

Zhang et al. [25] studied material flow line control in isothermal precision forging by combining experiment with FEM simulation. Flow lines distribution agreed with the simulation of FEM. It was expressed in study that the radial flow lines distribute along the forging shape more easily than the axial flow lines do.

Petrov et al. [26] described a research about an aluminum part with a deep central cavity and irregular shape of on isothermal enclosed die forging. They were used QFORM-3D FE software package for forging simulations and carried out experimental studies. They showed that the simulation results were in good agreement with experimental ones.

Pillinger et al. [27] studied the mathematical formulation of FE numerical simulation of forging process. They were focused on the material phenomena, computational aspect, interface phenomena on the die design and process modelling.

Park et al. [28] presented the analysis of multistage forging process for low production cost and fast production of complex shaped part with no flash. FEM was used for analyzing the process in terms of the die load, the velocity fields, the effective strains and shapes of preforms.

2.3 The Contribution of the Study

This thesis investigates the process design for enclosed die forging combined with bi-directional and bi-directional step motions realized using servo-press machine with the aid of FEM. Especially while using the servo-press machine for the forging process, the application of numerical simulation is essential to achieve reliable process design, as it can provide useful information to overcome the difficulties associated with the increase in flexibility and complexity of servo-press motion control [20]. In order to reduce the forging load and to obtain complete die filling, bi-directional step forgings (divided-flow method) were performed with two upper and two lower punches die sets. Upper and lower punches are moving first to reach the final height of the forging then the upper and lower rings are moving to complete the forging operation. On the basis of the simulation and experimental results obtained, it can be realized that the process design introduced in this thesis can provide useful information on the effect of forging process using servo-press with bi-directional and bi-directional step motion definition.

CHAPTER 3

ENCLOSED DIE FORGING AND FINITE ELEMENT METHOD

3.1 Enclosed Die Forging

Metal forming, as a fundamental process, has been used for thousands of years. Machinery, tooling and materials using are well-developed in metal forming in years to make new technologies and improvements of products. Forging is a metalworking process used to shape metal by hammering or squeezing under compressive forces. It is preferred due to high productivity and proper fiber orientation which improves the mechanical properties of the product. Despite of these advantages, forging technology is in tough competition to other processes, such as casting, sintering or machining. The cost effectiveness and the quality requirements of the final product are the two main factors in selection of the manufacturing process.

In the last fifty years period, precision forging technique has been developed as a near-net shape process. Precision forging can be defined as a completely closed die flashless forging which generates high quality parts with required surface finish and dimensional accuracy.

Fully-enclosed die forging is a precision forging process that has been developed since the 1970s, which uses one-ram or multi-ram as punches to press the billet in a pre-enclosed die to form a complicated shape forging without flash. [29]. The name of “enclosed die forging” was given due to closing the die cavity during forging and opening when the product is taken out [30].

Enclosed die forging can be carried out as hot, cold or warm process in complex shape parts. The volume of metal part can be controlled within very narrow limits to achieve complete filling of the cavity without developing extreme pressures. It takes some very well controlled preforming steps to accomplish this precise weight control in the final die.

One of the important characteristic of enclosed-die forging is usage of multiple-action punches in a pre-enclosed die to fill the die cavity (see Figure 3.1). The metal flow can be controlled to obtain the required flow pattern by controlling the motion of rams. The motions of upper and lower punches may be set as synchronous, asynchronous, or with back pressure to reduce forming load or to improve the filling of material [31]. Some of the advantages of enclosed-die forging are:

- The ability to forge complex shapes in one process
- Higher material utilization due to elimination of flash and subsequent machining operations (either reduced or, in some cases, eliminated)
- Reducing forging load by decreasing the area penetrated by the punch [32].

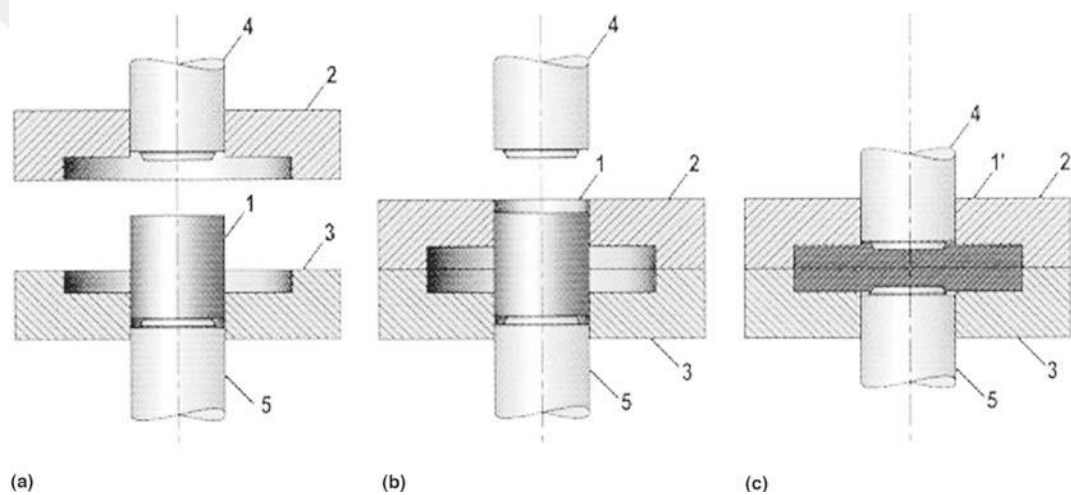
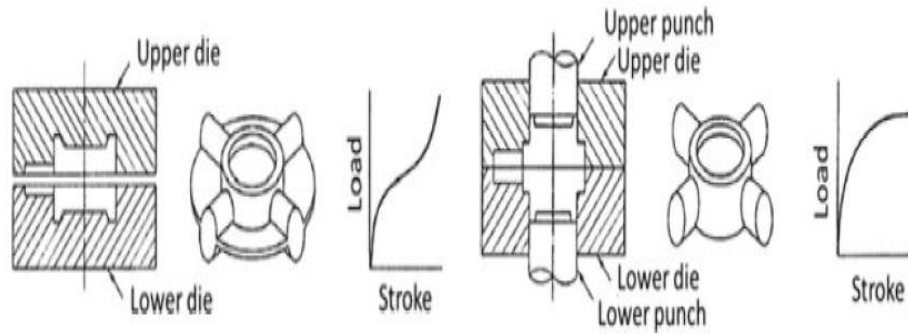


Figure 3.1 Enclosed-die forging. 1, billet; 2, upper die; 3, lower die; 4, upper punch; 5, lower punch; 1', finished part [31]

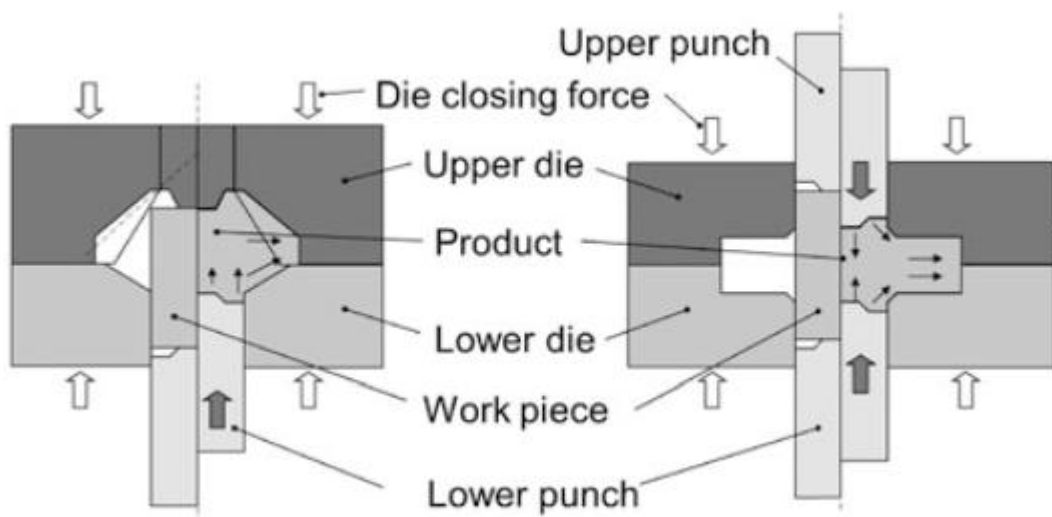
A comparison of conventional semi-closed die forging and enclosed die forging processes for producing a cross pin is given in Figure 3.2 [33]. The difference between the load-stroke diagrams shows that the forging load increases asymptotically as deformation proceeds and large thin burr is formed (larger contact area) in classical closed die forging. Note that, further additional cutting of the burr and machining of the extruded rods are required.



(a) Classical semi-closed die forging (b) Enclosed die forging of cross pin

Figure 3.2. Comparison of a) classical semi-closed die forging and b) enclosed die forging of cross pin [33].

In the case of enclosed die forging, the forging load is lower because the contact area between the punches and the workpiece interface is limited to the punch ends during the whole process. This example shows the advantages of enclosed die forging for forging of dimensionally accurate products. Figure 3.3 shows two more practical examples of enclosed die forging. In bevel gear and inner race forgings one moving punch is used. For cross pin and tripod forgings two moving punches, the die closing mechanism, and usually three moving axes are required [34].



(a) One moving punch (b) Two moving punches

Figure 3.3. Enclosed die forging methods and products. **a** One moving punch, **b** Two moving punches

3.2 Presses for Enclosed Die Forging

In order to facilitate the enclosed die forging, press builders have developed multi-action and servo-driven presses. In a multi-action press, there is more than one pressure source to move the slides and dies. Also, the dies can make several relative motions during one stroke. A schematic view of multi-action press and helical gear forging die set is given in Figure 3.4.

A servomotor press that combines a newly developed large-sized, high torque servomotor drive with a crank mechanism is shown in Figure 3.5. The press is controlled by the aid of computer to obtain high functionality. Therefore, it is possible to set the optimum parameters required to form the part by input the movement and speed of the die components (see Figure 3.6). This may be used advantageously to produce hard to- form materials and increase die life.

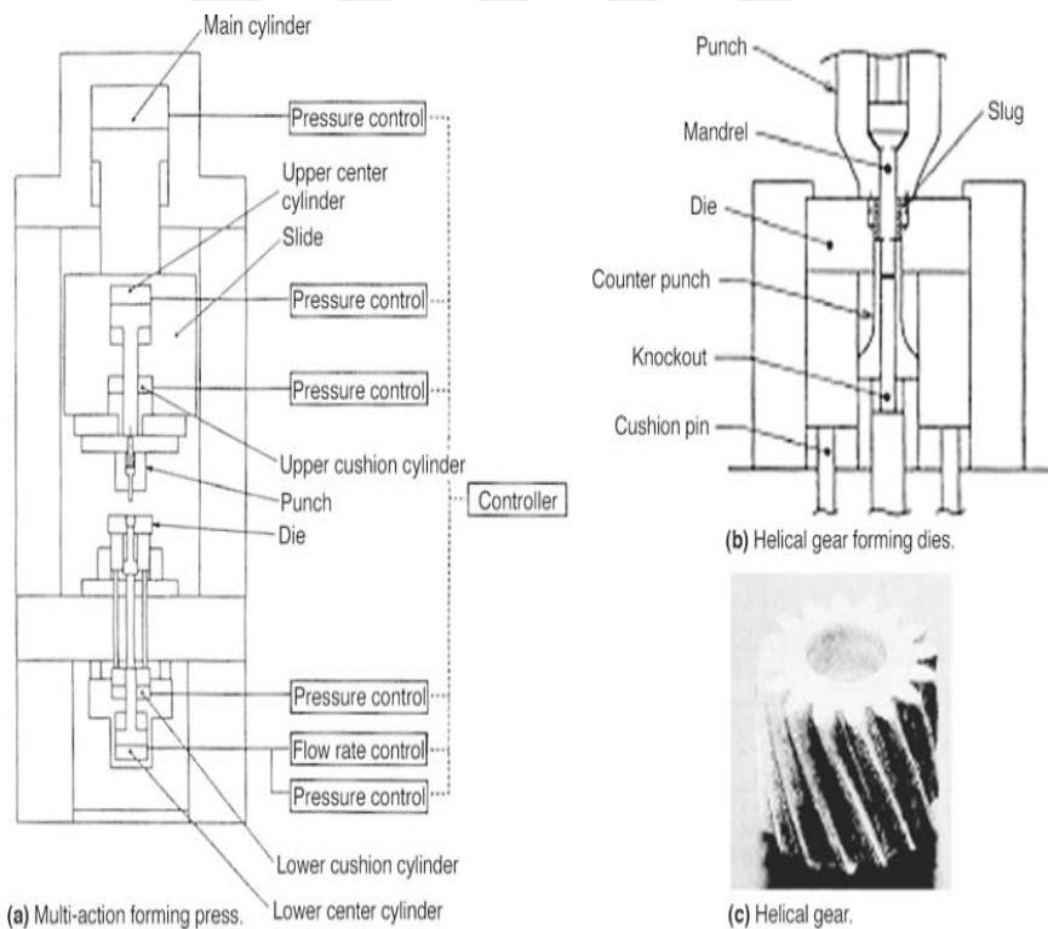


Figure 3.4 Multi-action presses [35]

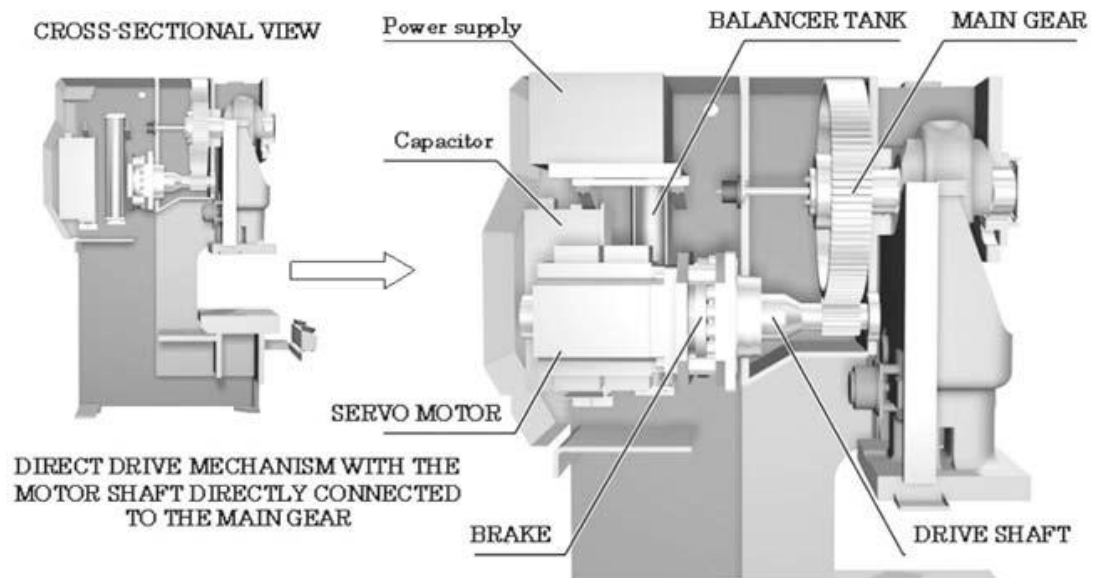


Figure 3.5 Sectional view of the drive mechanism of the Aida Digital Servo Former [36]

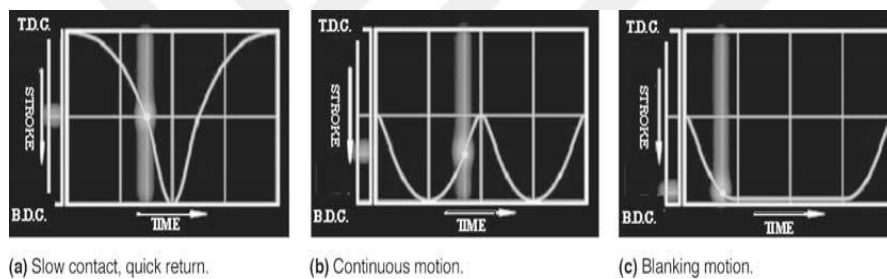


Figure 3.6 Some example settings of forming motions and speeds. [36]

3.3 Finite Element Method (FEM)

Finite element analysis (FEA) has been developed during the last decades as a very useful tool for analysis of metal forming processes. Progress in development of cheap and efficient computer technology. The implementation of the finite element method (FEM) into user-friendly, window-based programs, has brought this technology forward. [37].

The finite element method (FEM) is a numerical technique whose basic concept is one of discretization. The FE model is generally constructed as follows. In the domain of the function a number of finite points are identified. The values of the function and its derivatives are specified at these points which are now called nodal points. The domain of the function is represented approximately by a finite collection of subdomains called finite elements. Then the elements are connected appropriately

on their boundaries in the assembly domain. The function is approximated locally within each element by continuous functions that are uniquely described in terms of nodal-point values associated with the particular elements. The solution of a finite-element problem consists of five specific steps: (a) identification of the problem; (b) definition of element; (c) establishment of the element equation; (d) the assemblage of element equations; and (e) the numerical solution of the global equations. The formation of element equations is accomplished from one of four directions (1) direct approach; (2) variational method; (3) method of weighted residuals; and (4) energy balance approach [38].

Looking back at the history of FEM, the usefulness of the method was first recognized at the start of the 1940s by Richard Courant, a German-American mathematician. While Courant recognized its application to a range of problems, it took several decades before the approach was applied generally in fields outside of structural mechanics.

One of the benefits of the finite element method (FEM) is that the theory is well developed. The reason for this is the close relationship between the numerical formulation and the weak formulation of the partial differential equation problem. For instance, the theory provides useful error estimates, or bounds for the error, when the numerical model equations are solved on a computer.

Another benefit of using the FEM is that it offers great freedom in the selection of discretization, both in the elements that may be used to discretize space and the basic functions. Discretization makes the model body by dividing it into an equivalent system of many smaller bodies or units (finite elements) interconnected at points common to two or more elements (nodes or nodal points) and/or boundary lines and/or surfaces (see Figure 3.7).

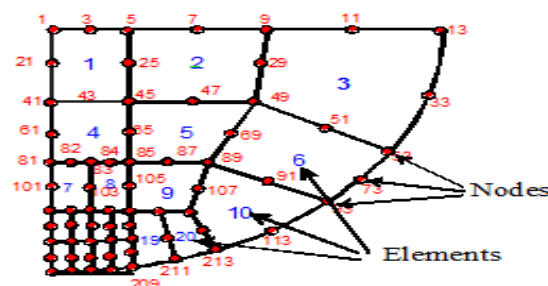


Figure 3.7 The elements and nodes formed by the process of discretization.

In recent years, the finite element method has been used to predict and analyze the material deformation during a metal forming operation. The following requirements should be executed to obtain successful finite element results.

1. Identify the physical problem
2. The idealization of this problem should be done correctly and assumptions and implications should be identified correctly.
3. Identify the correct spatial discretization conditions such as type of elements used, topology of element mesh, and the density of element mesh should be constructed according to the nature of problem.
4. Identify the boundary conditions applied in the simulation: friction, heat transfer, machines, dies etc.
5. Identify correct material laws and parameters such as flow curve, anisotropy, failure, etc.
6. Identify numerical parameters used in the simulation accordingly: penalty factors, convergence limits, increment sizes, remeshing criterion etc.
7. Optimization of the computational times, the time required to prepare the model and storage requirements of the model and the results are other important factors to obtain desired result. Also the simulation should be economical.
8. The results should be evaluated carefully and checked whether they are valid or not [39].

The main advantages of finite-element methods are: (1) the capability of obtaining detailed solutions of mechanics in deforming body, namely, velocities, shapes, strains, stresses, temperatures, or contact pressure distributions; and (2) the fact that a computer code, once written, can be used for a large variety of problems by simply changing the input data.

While many commercial finite elements software package programs are available, DEFORMTM is a Finite Element Method (FEM) based process simulation system designed to analyze various forming and heat treatment processes used by metal

forming and related industries. By simulating manufacturing processes on a computer, this advanced tool allows designers and engineers to:

- i) Reduce the need for costly shop floor trials and redesign of tooling and processes,
- ii) Improve tool and die design to reduce production and material costs,
- iii) Shorten lead time in bringing a new product to market.

A user friendly graphical interface provides easy data preparation and analysis so engineers can focus on forming, not on learning a cumbersome computer system. An essential component of this is a fully automatic, optimized remeshing system that is tailored for large deformation problems. [33]



CHAPTER 4

FE MODELLING AND EXPERIMENTAL STUDY

4.1 FE Modelling

The commercial finite element software package DEFORMTM has been used throughout the study. Unlike general purpose FEM codes, DEFORM is tailored for deformation modeling, so that it is very suitable for forging simulations. H-Shape forgings were chosen to simulate enclosed die forging of axisymmetric parts. Due to rotational symmetry of the H-Shape forgings carried out in the study, axisymmetric analyses used. The die components and workpiece were considered as rigid and elasto-plastic material, respectively. The friction model was taken as constant shear friction which is mostly used for bulk forming simulations [24]. The preform used in H-shape forging simulations is a hollow cylinder and the dimensions of the preform and the final forging geometry are given in Figure 4.1. The dimensions of the hollow preforms are calculated from the final forging using the volume constancy. For the models; 5100-5600 elements were generated depending on the geometry by using the automatic mesh generation. Lagrangian incremental type and the Newton-Raphson Method were used for the solver and the iteration method, respectively. DEFORM uses AMG (Automatic Mesh Generator) to solve problems of large deformation and to automatically provide an optimized re-meshing capability.

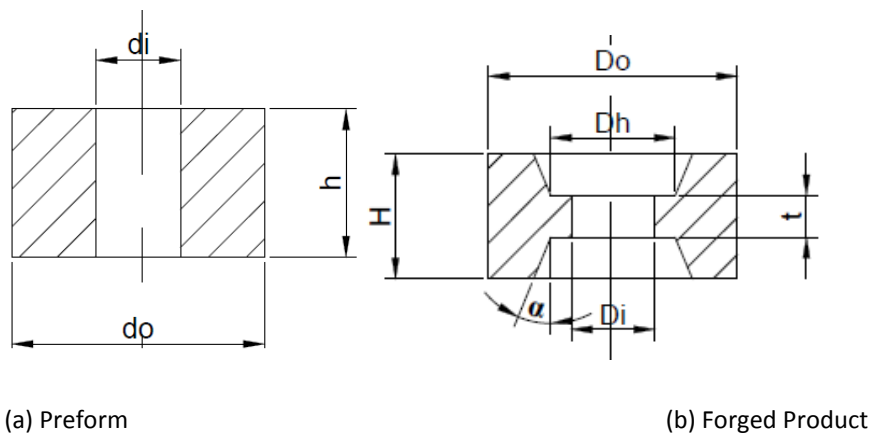


Figure 4.1 Geometric Model of H-Shaped (a) Preform (b) Forged product

4.1.1 H-Shaped Part Geometry

Final height (H), hub diameter (D_h), outer (D_o) and inner (D_i) diameters of the H-shape forgings are taken as 15mm, 15mm, 30mm and 10 mm, respectively for all forgings. Hub thickness (t) and rib angle (α) are variables as parameters shown in Figure 4.2. The values of these parameters are given in Table 4.1.

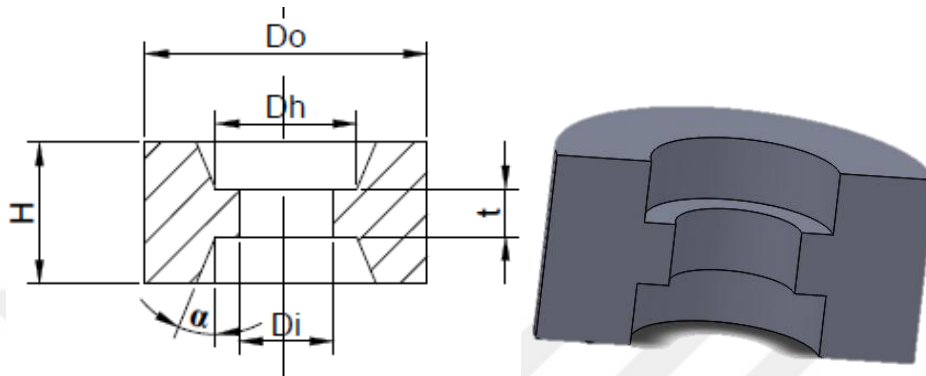


Figure 4.2 Geometric Model of Forged H-Shaped Products

Table 4.1 Dimensions of variables of Preforms and H-Shape Forgings

H-SHAPE FORGING PART NO	Rib Angle (α)($^{\circ}$)	Hub Thickness (t)(mm)	P1(Preform 1) d_i/d_o (17/30)mm Heights(h)(mm)	P2 (Preform 2) d_i/d_o (10/30)mm Heights(h)(mm)
H1	0	5	17,60	13,44
H2	1	5	17,56	13,41
H3	3	5	17,47	13,34
H4	7	5	17,29	13,21
H5	14	5	16,96	12,95
H6	22	5	16,52	12,62
H7	26	5	16,27	12,43
H8	45	5	14,60	11,15
H9	0	7,5	18,11	13,83
H10	26	7,5	17,38	13,28
H11	45	7,5	16,50	12,61
H12	0	10	18,62	14,22
H13	26	10	18,31	13,98
H14	45	10	17,94	13,70

4.1.2 Preform Geometry

The outer diameter (d_o) of preform is equal to the H-Shape forgings ($\text{Ø}30 \text{ mm}$). The heights (h) and the inner diameter (d_i) of preforms are calculated from corresponding H-Shape forgings using volume constancy. The preforms are simple hollow cylinders are shown in Figure 4.3. The corresponding dimensions of the preforms are given in Table 4.1.

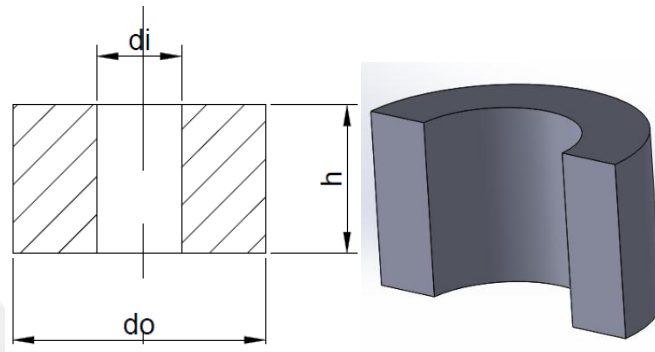


Figure 4.3 Geometric Model of Preforms for H-Shape Forging

Two types of preforms P1 and P2 were used in study to compare upsetting and extrusion modes of metal flow as shown in Figure 4.4. If the movement of punch and the material flow are perpendicular to each other, the deformation mode is called upset mode. If the movement of punch and the material flow are parallel to each other, the deformation mode is named as extrusion mode.

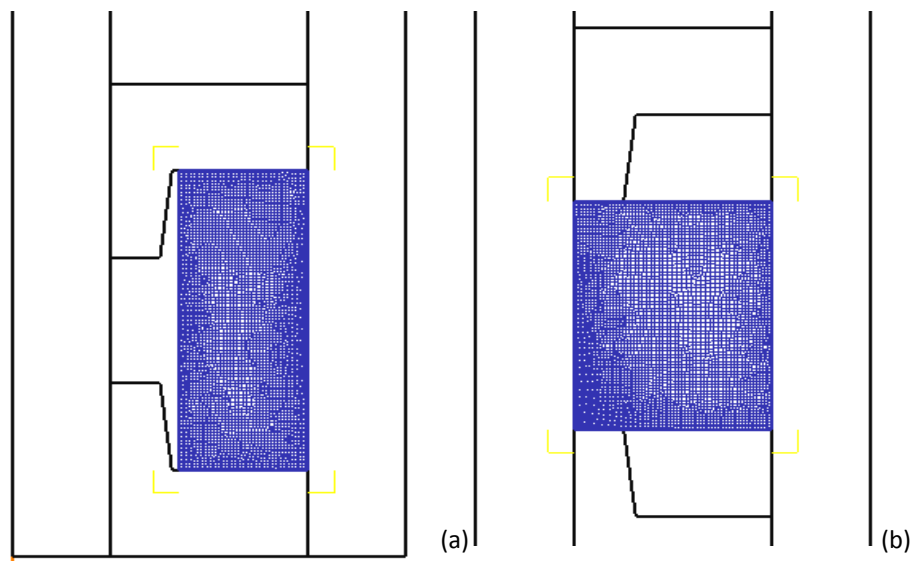


Figure 4.4 a)Preform P1 $d_i=17 \text{ mm}$ upset mode of metal flow b)Preform P2 $d_i=10 \text{ mm}$ extrusion mode of metal flow

4.1.3 The Loading Conditions

Three loading conditions were performed as they called uni-directional, bi-directional and bi-directional step of initial and final FE model as shown in Figure 4.5 and Figure 4.6 for two different preforms for upset and extrusion modes. Because of symmetry, only right one side of the workpiece was used for the FEM simulation model to reduce the calculation time.

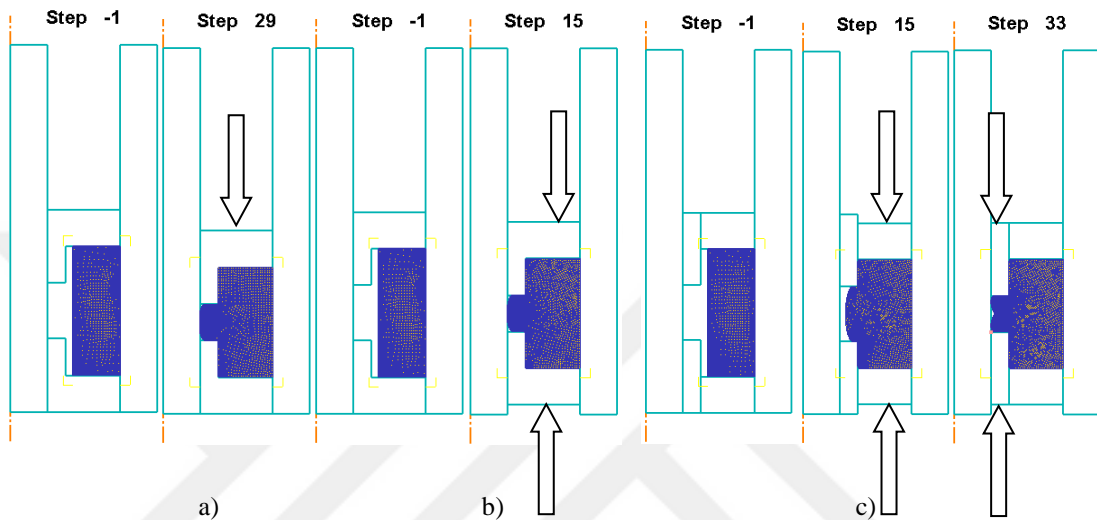


Figure 4.5 FE Model of H-Shaped upset mode forging (P1) of initial and final step of three loading conditions; a) uni-directional, b) bi-directional c)bi-directional step

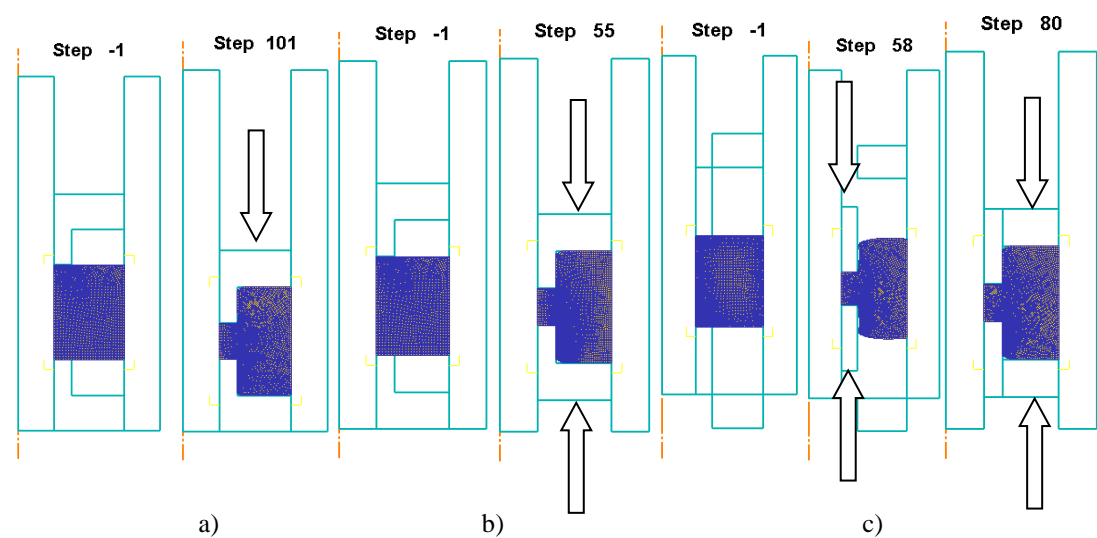


Figure 4.6 FE Model of H-Shaped extrusion mode forging (P2) of initial and final step of three loading conditions; a) uni-directional, b) bi-directional c)bi-directional step

The speed of the top and bottom dies were chosen as 0 mm/s and 1 mm/s according to uni-directional and bi-directional loading conditions and the speed of top ring and bottom ring were chosen as 0 mm/s and 1 mm/s according to bi-directional step.

4.1.4 Preform Material

Two materials plasticine and Al 1100 were used for preform in this study. Plasticine was used for verifications of FE model by experimental study. The FE simulations were carried out for Al 1100. The flow curve of Al 1100 was taken from DEFORM™ database and it is shown in Figure 4.7.

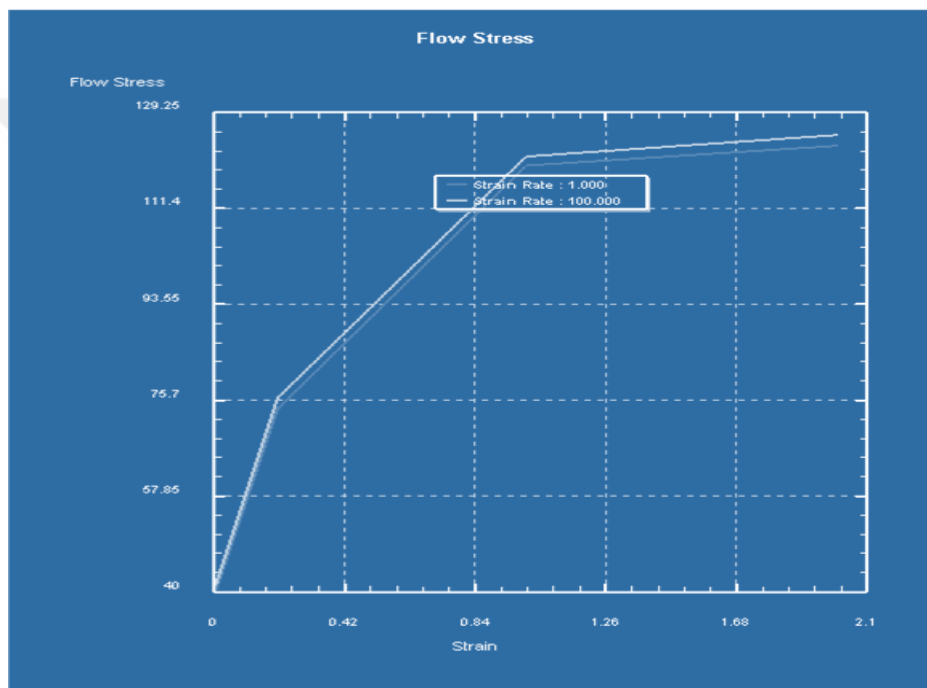


Figure 4.7 The Flow Curve of Aluminum 1100 taken form DEFORM database

4.2 Experimental Study

4.2.1. The Modeling Material and Plasticine Specimen Preparation

A physical modeling technique was used for verification of the FE simulation. For this purpose, commercially available plasticine was chosen as a modeling material by considering the servo-press capacity used in the study. Due to the capacity limitation (20 kN) of the servo-press used in the study, plasticine was chosen as a modeling material. The slabs of plasticine were heated to 50⁰ C in order to make it softer. Then, they were worked by repeated rolling and folding to obtain a reasonable homogeneity.

The plasticine dough was filled into glass tube having 30 mm internal diameter and 50 mm length. The internal surface of the tube was dusted with talcum powder prior to filling to prevent sticking. Once the tube was completely filled, the cylindrical Plasticine was pushed out from the tube and the both ends (top and bottom) were cut out to minimize the end effect and leave the height of the middle segment as 30 mm. This middle segment was used for compression tests in order to determine the flow stress of the Plasticine material. The Plasticine preforms for the H-shape forgings were prepared similarly. In this case, a 17 mm diameter mandrel was replaced into the center of the glass tube to obtain hollow preforms. The plasticine was pushed out from the tube together with the mandrel. The both ends were cut out to obtain 17,6 mm height hollow preforms. Then the mandrel was removed gently to keep the shape.

4.2.2 Compression Test

In compression testing of the plasticine specimens, two plexiglass platens were used as top and bottom die. The surface of the specimens and the plexiglass platens were lubricated with talcum powder to reduce the friction at the interface. The barreling of the specimens during testing was very small, so that the friction effect was almost eliminated. Shimadzu AGX tension/compression testing machine was used with a loading velocity of 1 mm/sec. The top platen was moving while the bottom one was fixed. The tests were repeated for 10 specimens at room temperature and the load-stroke diagram was obtained. The flow curve was calculated by using the well-known true-stress true-strain equations:

$$\sigma_t = \sigma(1 + \epsilon) \quad (4.1)$$

$$\epsilon_t = \ln(1 + \epsilon) \quad (4.2)$$

4.2.3 Forging Press and Die Set

The photograph of the servo-press is shown in Figure 4.8 and the sketch of the die set used in the study is given in Figure 4.9. The press has two movable punches (top and bottom) which are driven by two separate servo motors. The die (container) is fixed on the press bed. The maximum capacity of the press is 20 kN and it is equipped with load cells and linear encoders to plot load-stroke diagram. The H-shape forging die set has three main parts; a die (container), top and bottom punches. They are all made of plexiglass and the dimensions are same as the die components used in FE simulations.



Figure 4.8 Photograph of the servo-press used in forging experiment

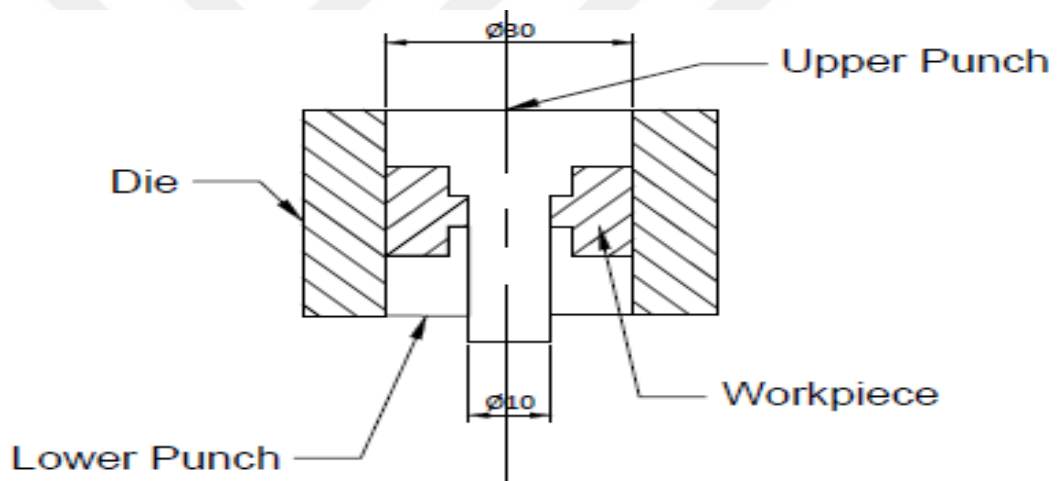


Figure 4.9 Sketch of the die set

4.2.4 H-Shape Forging of Plasticine

The plasticine hollow preforms were forged to H-shapes (H1) by using the servo-press and the plexiglass die set. Talcum powder was used as the lubricant in the forging processes. The speeds of the top and bottom dies were chosen as 0 and 1 mm/s according to uni-directional, bi-directional and bi-directional step loading conditions.

CHAPTER 5

RESULTS AND DISCUSSION

5.1 Experimental Results

5.1.1. Compression Test and Flow Curve of Plasticine

The load-stroke diagram of the plasticine specimens in the compression test is given in Figure 5.1. The flow stress curve of the plasticine was calculated using Eqs. (4.1) and (4.2). It is shown in Figure 5.2.

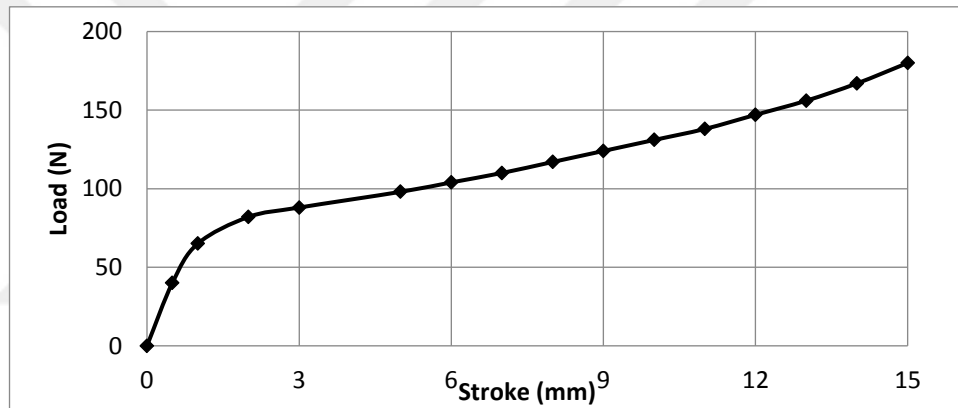


Figure 5.1 The load-stroke diagram of the plasticine specimens in the compression test.

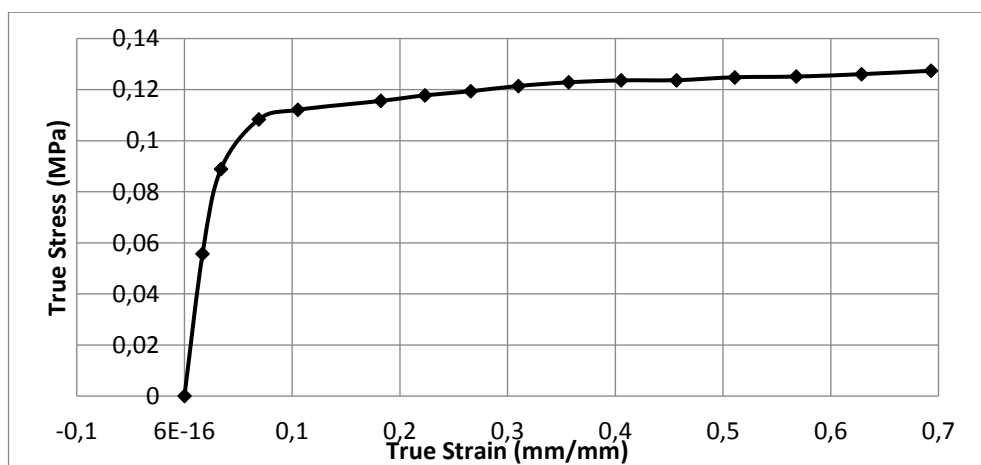


Figure 5.2 The flow stress curve of the plasticine.

5.1.2 H-Shape Forging of Plasticine

The load-stroke diagrams of H-shape forgings for (H1) for uni-directional and bi-directional loading conditions are shown in Figure 5.3. The curves have secondary mode of increasing the load after (1,6 mm for uni-directional and 0.8 mm for bi-directional) movement of the punch(es) where the inner portion of the H-shape start to fill. The maximum forging load in bi-directional loading is lower than uni-directional case.

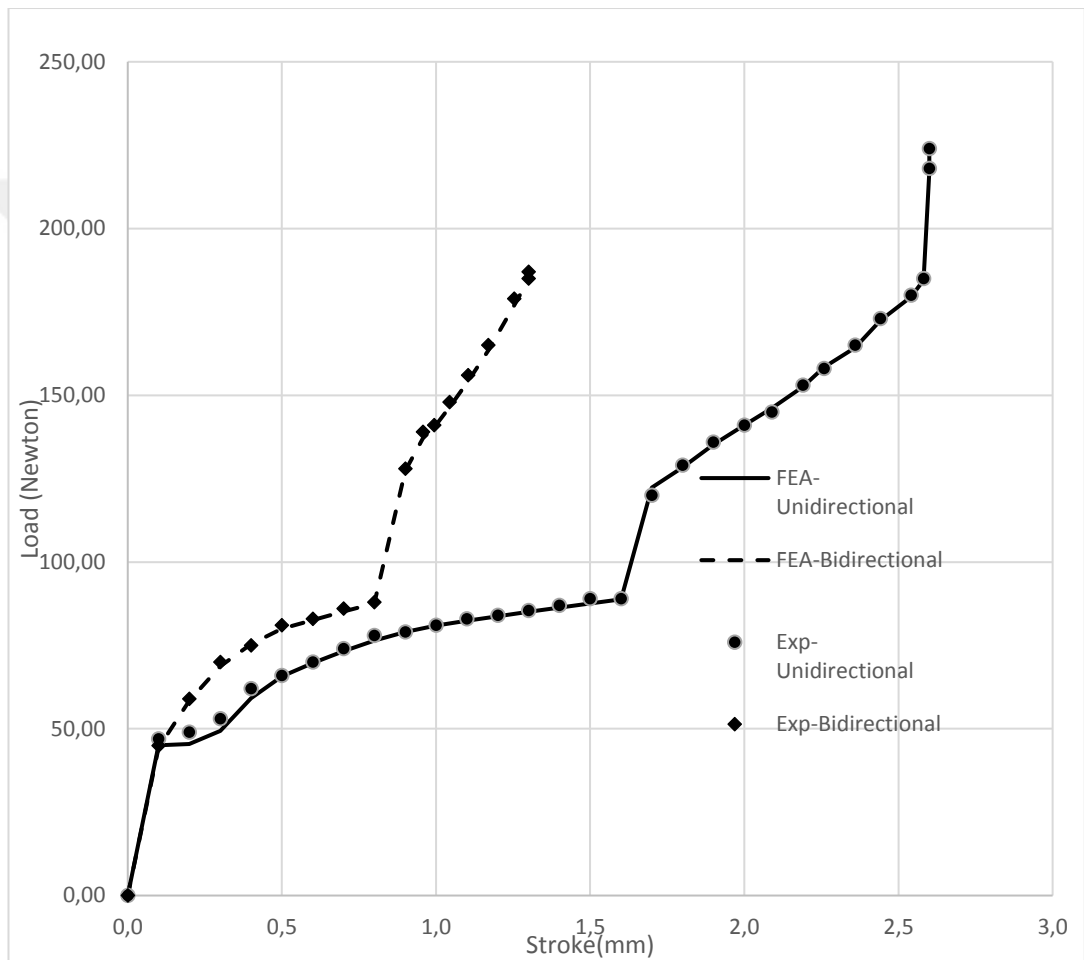


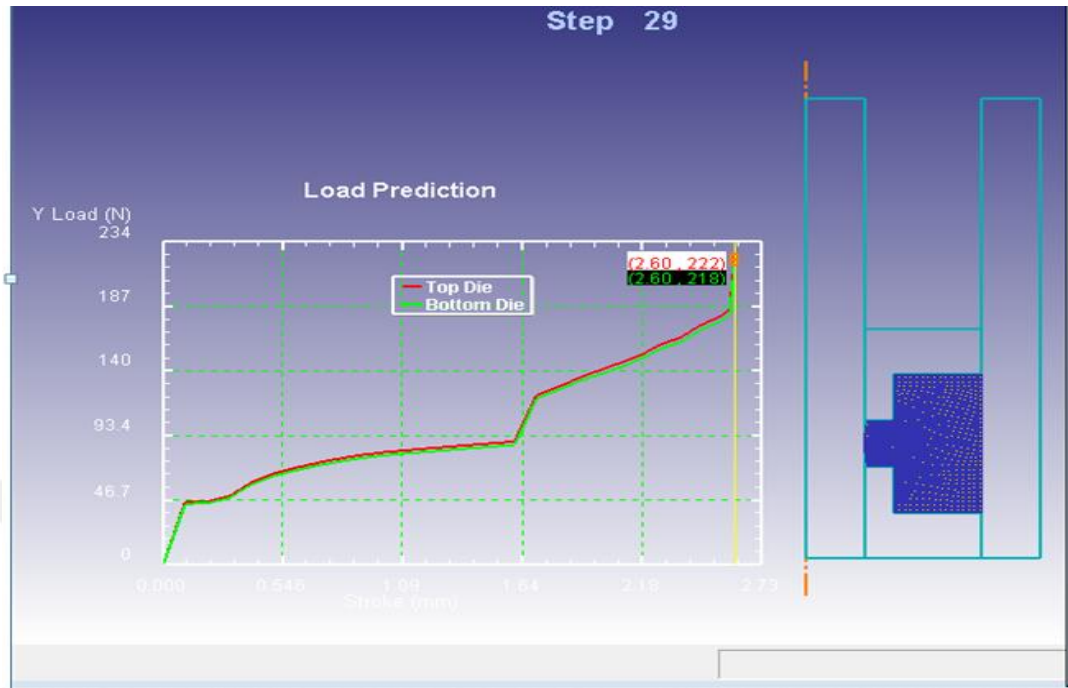
Figure 5.3 Experimental and FE load-stroke diagram of H-Shape plasticine forgings.

5.2. FE Results

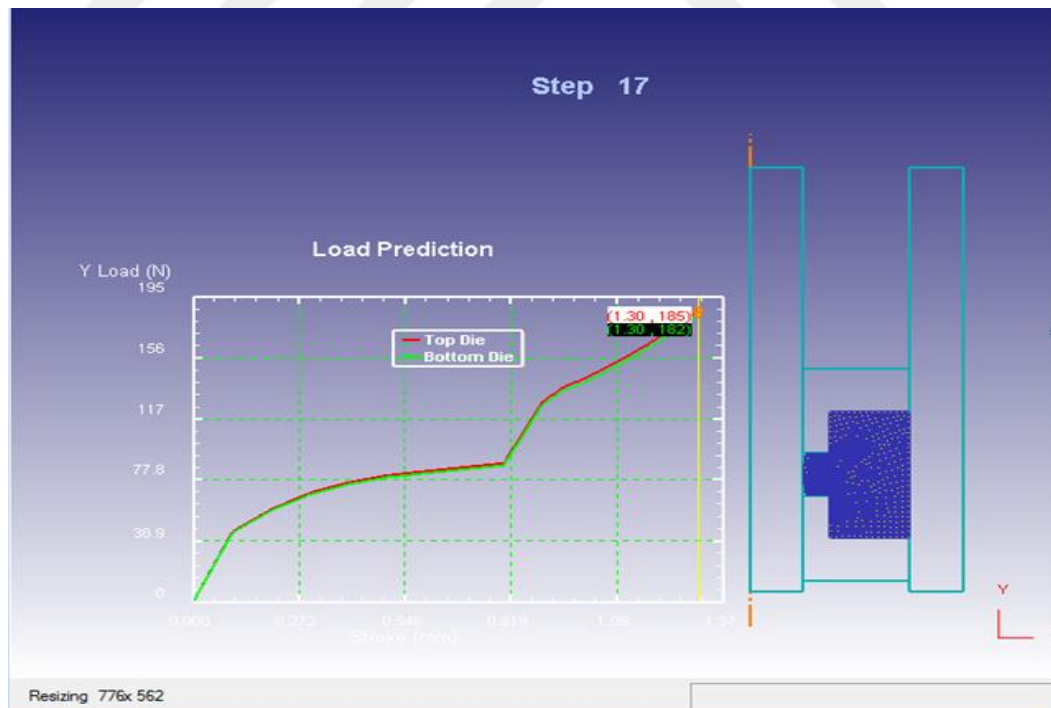
5.2.1 Plasticine Simulations

The flow stress curve obtained from the compression test results were used in the FE simulations as the material data. The friction coefficient was taken as 0.01. The load-stroke diagram. The flow of material obtained from the FE simulations results are

given in Figure 5.4. The results have shown a very close agreement with the experimental ones. This is validated in the FE simulations.



(a) Uni-directional Loading



(b) Bi-directional loading

Figure 5.4 The FE output of plasticine H-shape forgings, a) Uni-directional b) Bi-directional loading.

5.2.2 Aluminum 1100 Forgings

The Finite Element simulations were carried out for H-Shape forgings using Al 1100 preforms (P1 and P2) given in Table 5.1 as shown the effect of uni-directional and bi-directional loading conditions. The forging energy consumption for friction ($m=0$) and ($m=0.4$) are shown in Table 5.2.

Table 5.1 Al 1100 Forging Load Results of Simulations

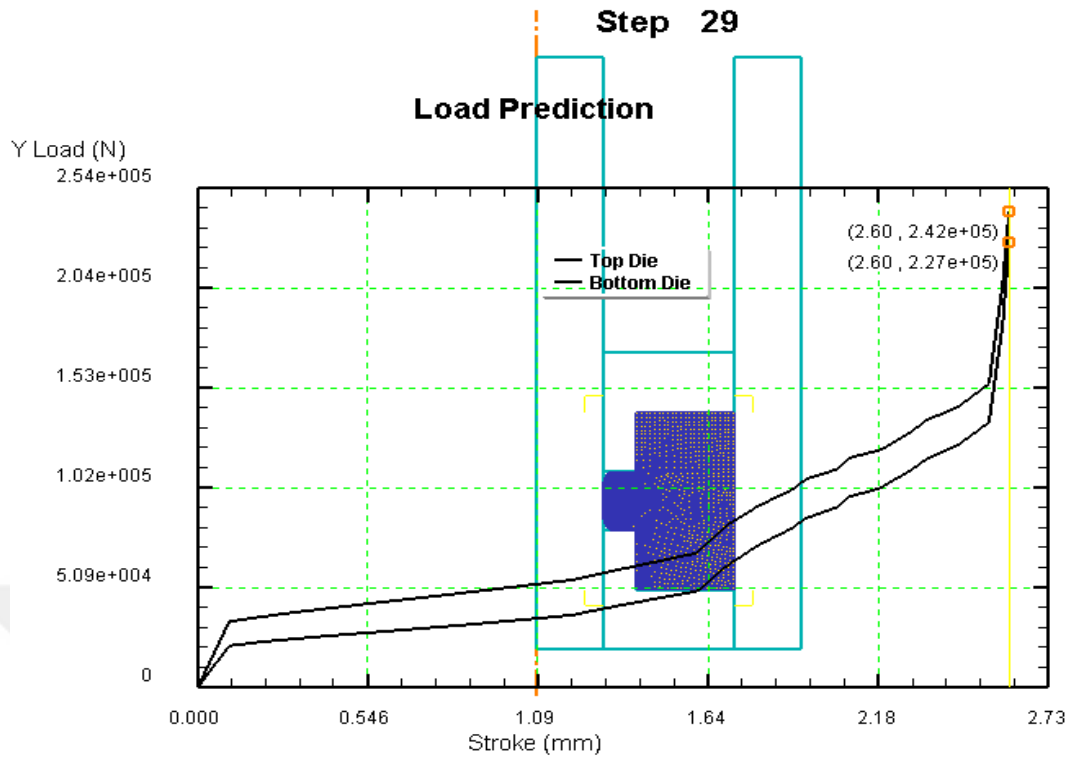
FORGING PART NO	Rib Angle (α)($^{\circ}$)	Hub Thick- ness (t) (mm)	P1 UNI- DIRECTIONAL FORGING LOAD ($m=0/m=0.4$) (ton)		P1 BI- DIRECTIONAL FORGING LOAD ($m=0/m=0.4$) (ton)		P2 UNI- DIRECTIONAL FORGING LOAD ($m=0/m=0.4$) (ton)		P2 BI- DIRECTIONAL FORGING LOAD ($m=0/m=0.4$) (ton)	
H1	0	5	19,50	24,20	16,60	21,20	18,40	19,60	18,40	19,00
H2	1	5	22,20	25,10	19,10	22,00	18,70	19,00	19,00	19,00
H3	3	5	22,00	24,30	20,10	21,70	17,00	17,80	17,50	18,00
H4	7	5	21,20	24,50	20,40	23,70	18,50	19,80	18,70	19,60
H5	14	5	24,60	28,20	24,40	28,80	18,30	20,20	19,60	19,90
H6	22	5	23,40	26,10	23,60	25,90	18,60	21,00	19,00	19,50
H7	26	5	22,30	26,30	23,40	26,70	18,20	20,90	18,60	18,60
H8	45	5	26,20	28,60	25,60	27,50	15,60	22,80	16,40	20,50
H9	0	7,5	20,30	25,10	18,70	22,50	18,30	19,80	19,20	19,60
H10	26	7,5	22,90	26,30	22,50	26,00	19,20	19,80	19,80	19,70
H11	45	7,5	25,20	28,60	25,10	28,70	23,10	27,70	23,50	22,20
H12	0	10	20,40	24,70	19,10	22,10	18,00	19,30	18,10	19,50
H13	26	10	21,50	27,00	22,40	26,10	17,70	18,10	18,00	18,60
H14	45	10	24,90	30,00	24,20	28,50	16,80	18,40	16,80	15,70

Table 5.2 Al 1100 Energy Consumption Results of Simulations

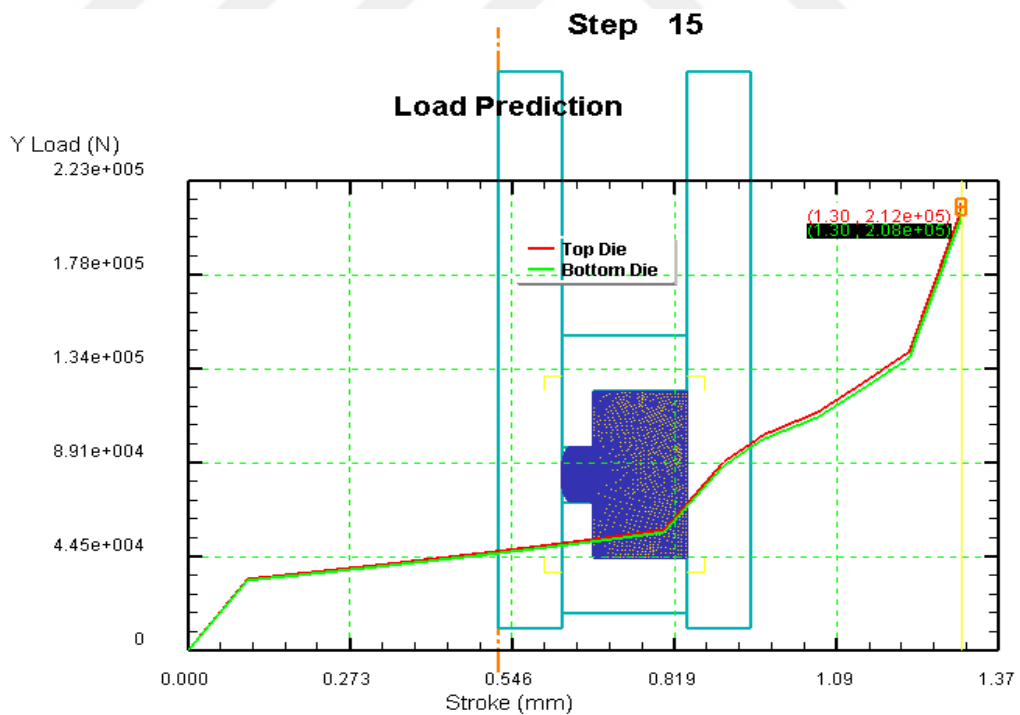
FORGING PART NO	Rib Angle (α)($^{\circ}$)	Hub Thick- ness (t) (mm)	P1 -UNI- DIRECTIONAL FORGING ENERGY (m=0/m=0.4) (j)		P1 -BI- DIRECTIONAL FORGING ENERGY (m=0/m=0.4) (j)		P2 -UNI- DIRECTIONAL FORGING ENERGY (m=0/m=0.4) (j)		P2 -BI- DIRECTIONAL FORGING ENERGY (m=0/m=0.4) (j)	
H1	0	5	160	194	156	181	229	296	234	246
H2	1	5	159	192	156	175	228	296	229	239
H3	3	5	158	183	155	174	227	292	225	244
H4	7	5	151	173	151	167	217	303	221	240
H5	14	5	147	168	150	165	216	311	221	252
H6	22	5	159	188	159	176	218	321	220	260
H7	26	5	168	205	168	190	219	325	221	260
H8	45	5	244	292	247	264	232	334	232	292
H9	0	7,5	193	235	191	220	160	210	162	172
H10	26	7,5	192	223	192	212	153	222	154	179
H11	45	7,5	235	276	237	260	168	241	174	202
H12	0	10	228	276	224	257	95	127	99	102
H13	26	10	227	265	227	253	92	130	93	106
H14	45	10	243	282	245	271	98	139	102	120

5.2.2.1 Effect of Loading Direction on Forging Load and Energy of Preform (P1) Upset Mode

The FE simulations were carried out for Aluminum 1100 preforms to show the effect of uni-directional and bi-directional forging processes. The load – stroke diagram and equivalent stress distribution for H1-P1 is given in Figure 5.5. The corresponding energy consumption H1-P1 is also given Figure 5.6.

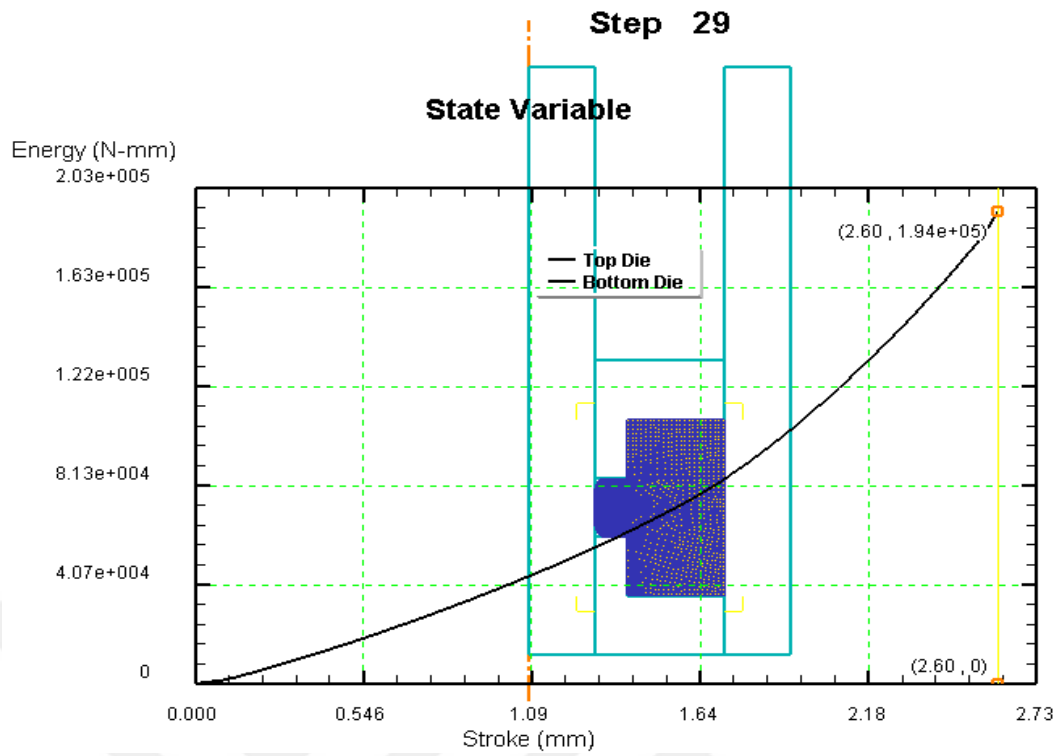


(a) Uni-directional forging

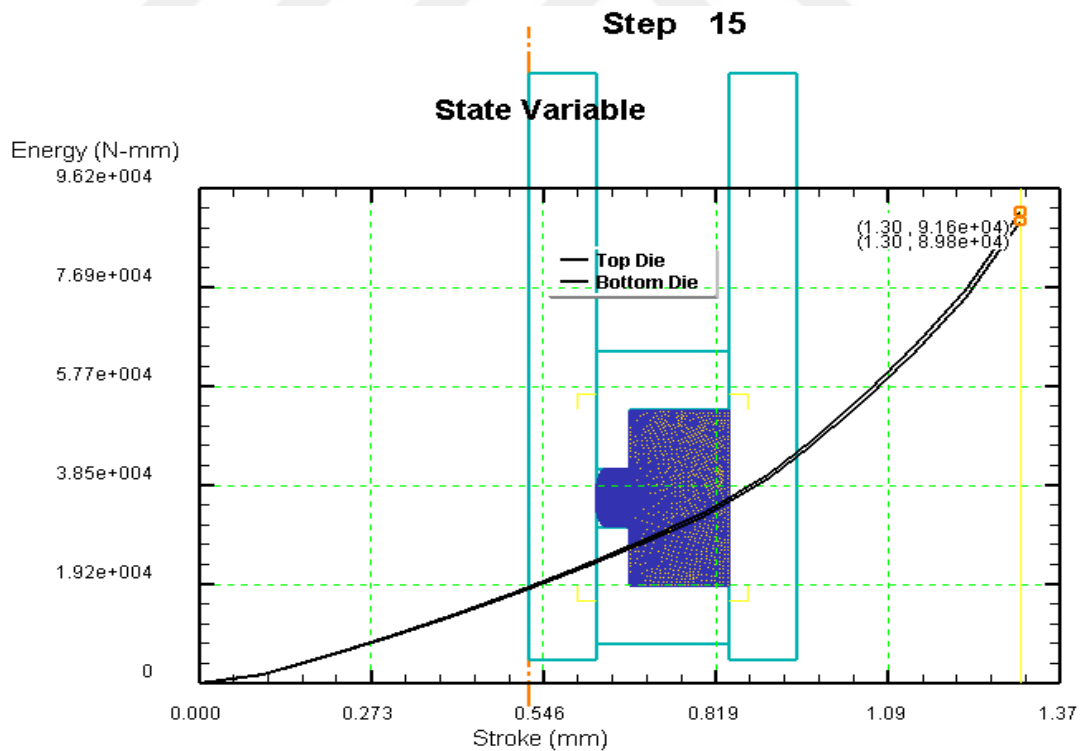


(b) Bi-directional forging

Figure 5.5 Forging load-stroke diagram and equivalent stress distribution of Aluminum 1100 H1-P1 for a) uni-directional forging and b) bi-directional forging.



(a) Uni-directional forging



(b) Bi-directional forging

Figure 5.6 Forging energies of H-shape Aluminum 1100 forgings H1-P1 for a) uni-directional and b) bi-directional loading.

The load-stroke diagram of H-shape forgings for various friction factors ($m=0-0.4$) are shown in Figure 5.7. The maximum forging load for various friction factor (m) is given in Table 5.3. As seen from the table, the maximum loads in uni-directional forgings were higher than bi-directional ones for all friction conditions.

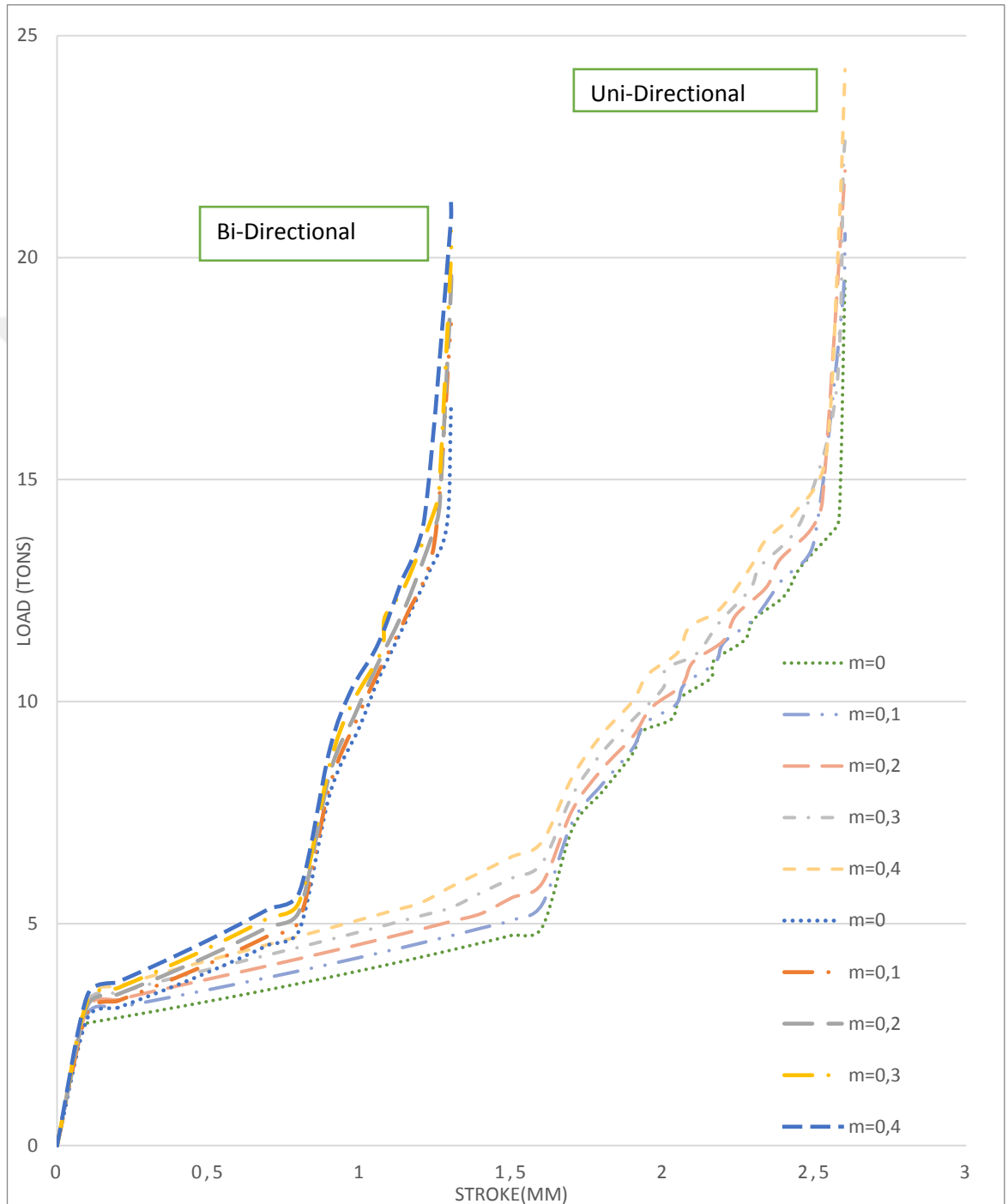
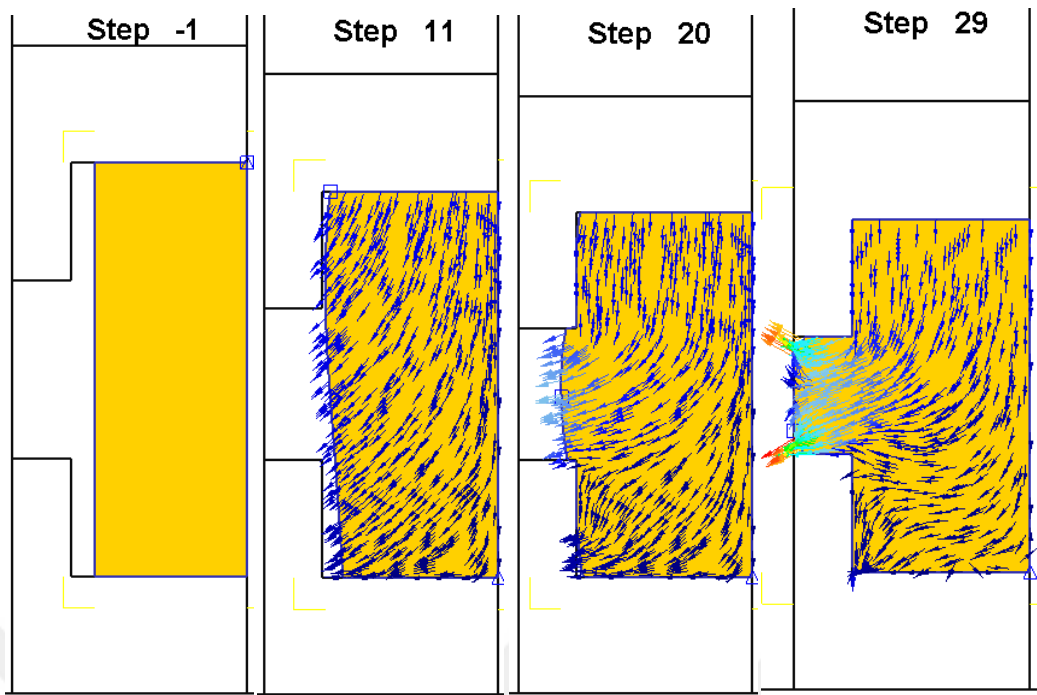


Figure 5.7 Uni-directional and Bi-directional forging loads for H1P1 with different friction factors (m).

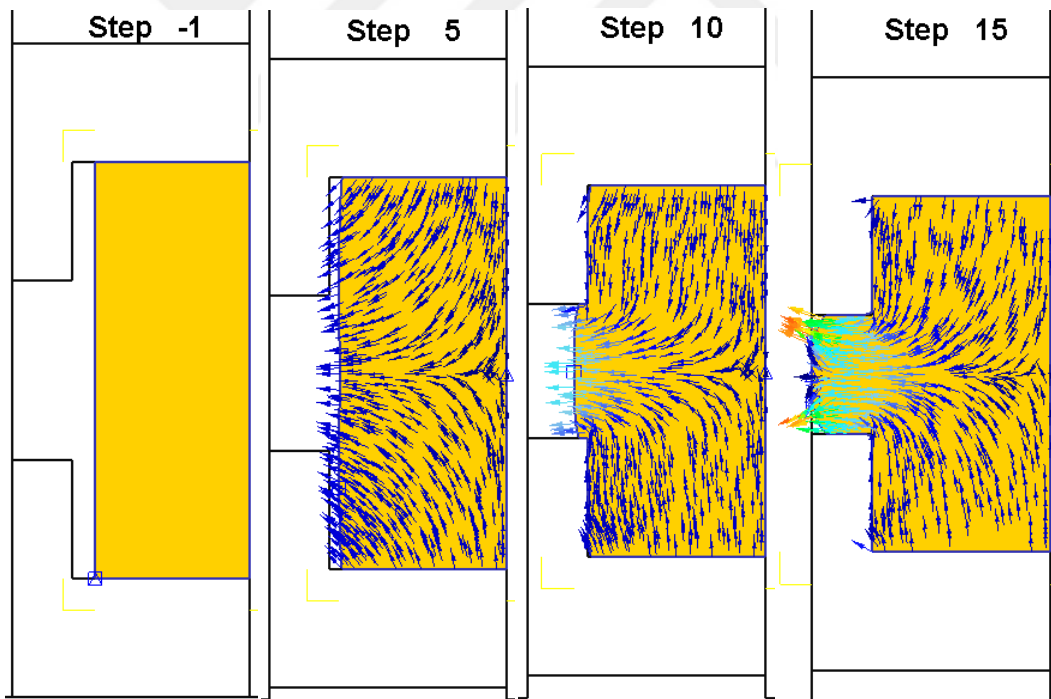
Table 5.3 The maximum Uni-directional and Bi-directional forging loads for various friction factor (m).

Friction Factor (m)	Al 1100 Simulation Max Load (Tons) for H1P1	
	Uni-Directional	Bi-Directional
0	19.58	16.65
0.1	20.54	18.50
0.2	21.96	19.92
0.3	22.67	20.60
0.4	24.24	21.21

The forging load is increased with the increasing friction at the billet-die interface. As seen from Table 5.3, the maximum loads in uni-directional forgings were higher than bi-directional ones for all friction conditions. This is due to the material flow pattern (see Figure 5.8). In bi-directional loading, the material flow is symmetrical, i.e., the top and bottom portion of the billet are flowing through the inner gap of the die. In the uni-directional loading case, the material at the top and the bottom are flowed differently through the inner gap. The material at the bottom is pressurized the inner die walls.



(a) Uni-directional Loading

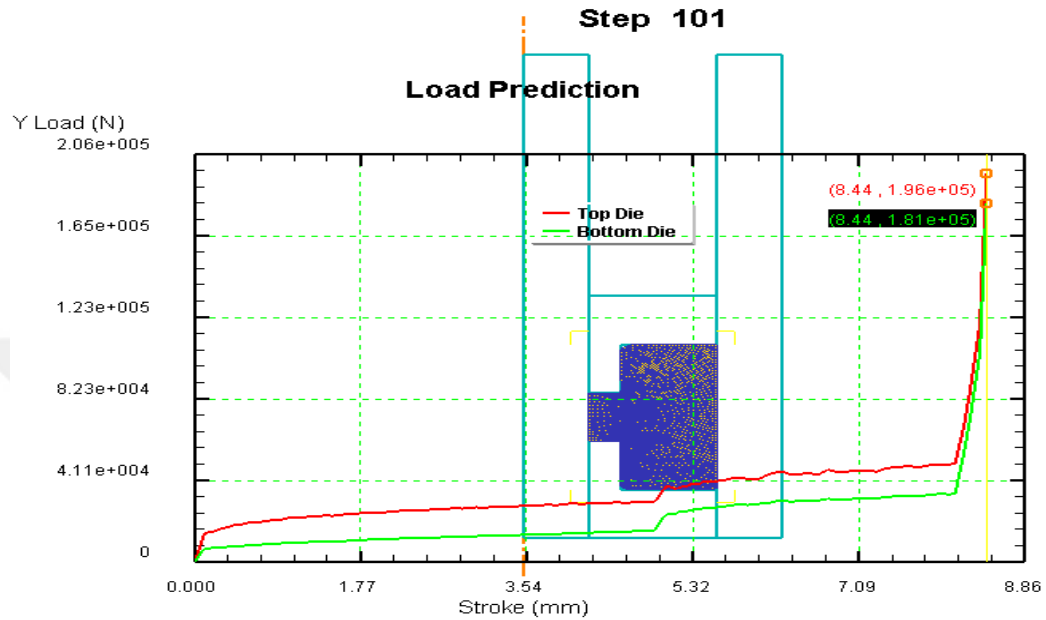


(b) Bi-directional loading.

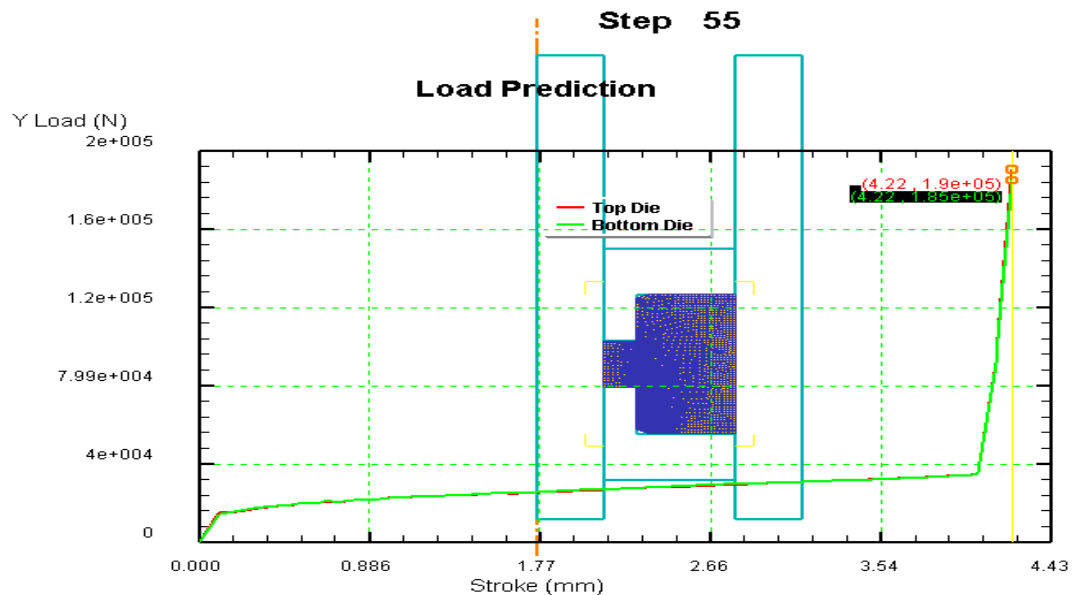
Figure 5.8 Upset mode of the material flow pattern of H1-P1 -shape Aluminum 1100 with friction factor ($m=0.4$) forgings for a) uni-directional and b) bi-directional loading.

5.2.2.2 Effect of Loading Direction on Forging Load and Energy of Preform (P2) Extrusion Mode

The load – stroke diagram and equivalent stress distribution for H1-P2 is given in Figure 5.9. The corresponding energy consumption H1-P2 is also given Figure 5.10.

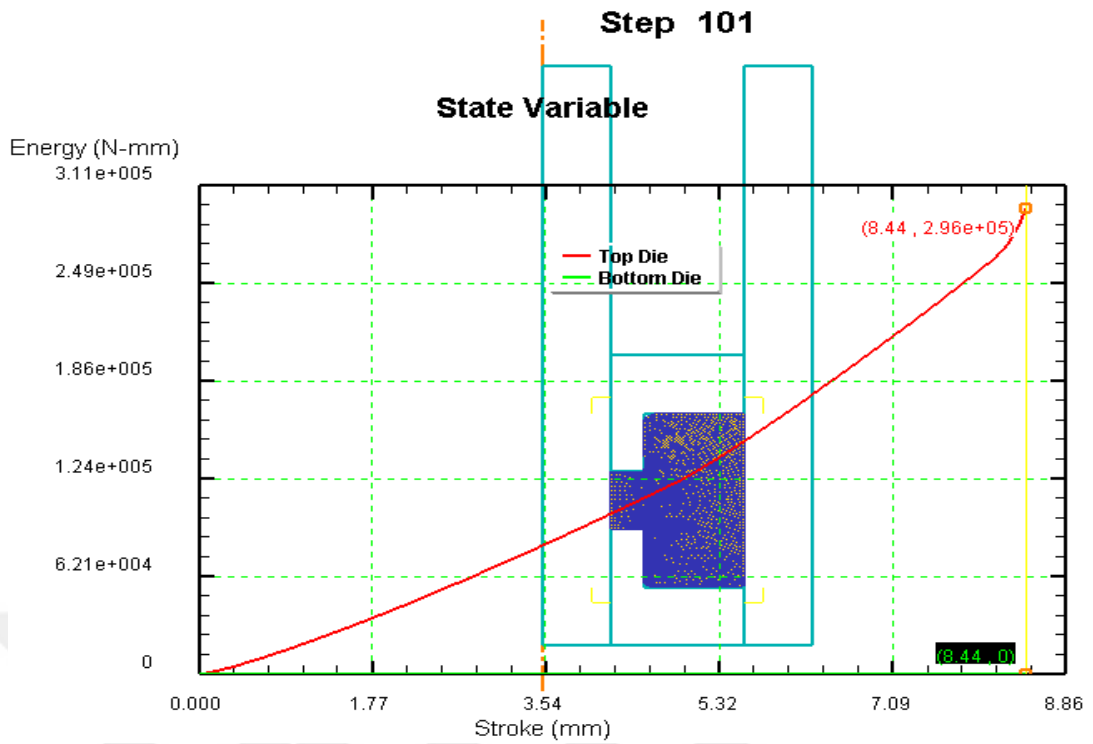


(a) Uni-directional forging

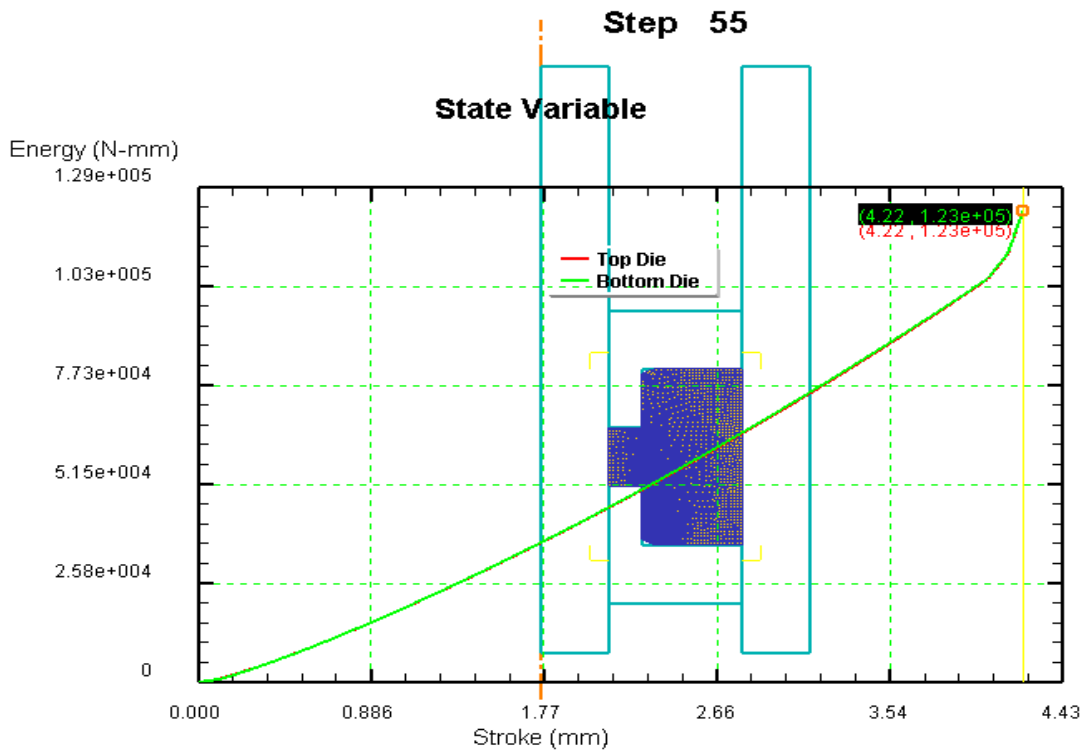


(b) Bi-directional forging

Figure 5.9 Forging load-stroke diagram and equivalent stress distribution of Aluminum 1100 H1-P2 for a) uni-directional forging and b) bi-directional forging.



(a) Uni-directional forging



(b) Bi-directional forging

Figure 5.10 Forging energies Aluminum 1100 forgings H1-P2 for a) uni-directional and b) bi-directional loading.

The maximum load is lower in bi-directional loading for $m=0.4$ than uni-directional loading. Comparing to preform P1, preform P2 requires lower forging load but higher energy due to longer stroke to fill the die cavity (See in Figure 5.11).

Extrusion mode of deformation where material flow and punch movement are parallel to each other, is easier than upset mode of deformation where material flow and punch movement are perpendicular to each other. The material flow for uni-directional and bi-directional forging of H1P2 are shown in Figure 5.12. In unidirectional forging of preform P2 the top part of the die is filled before the bottom die while symmetrical material flow is observed in bi directional forging.

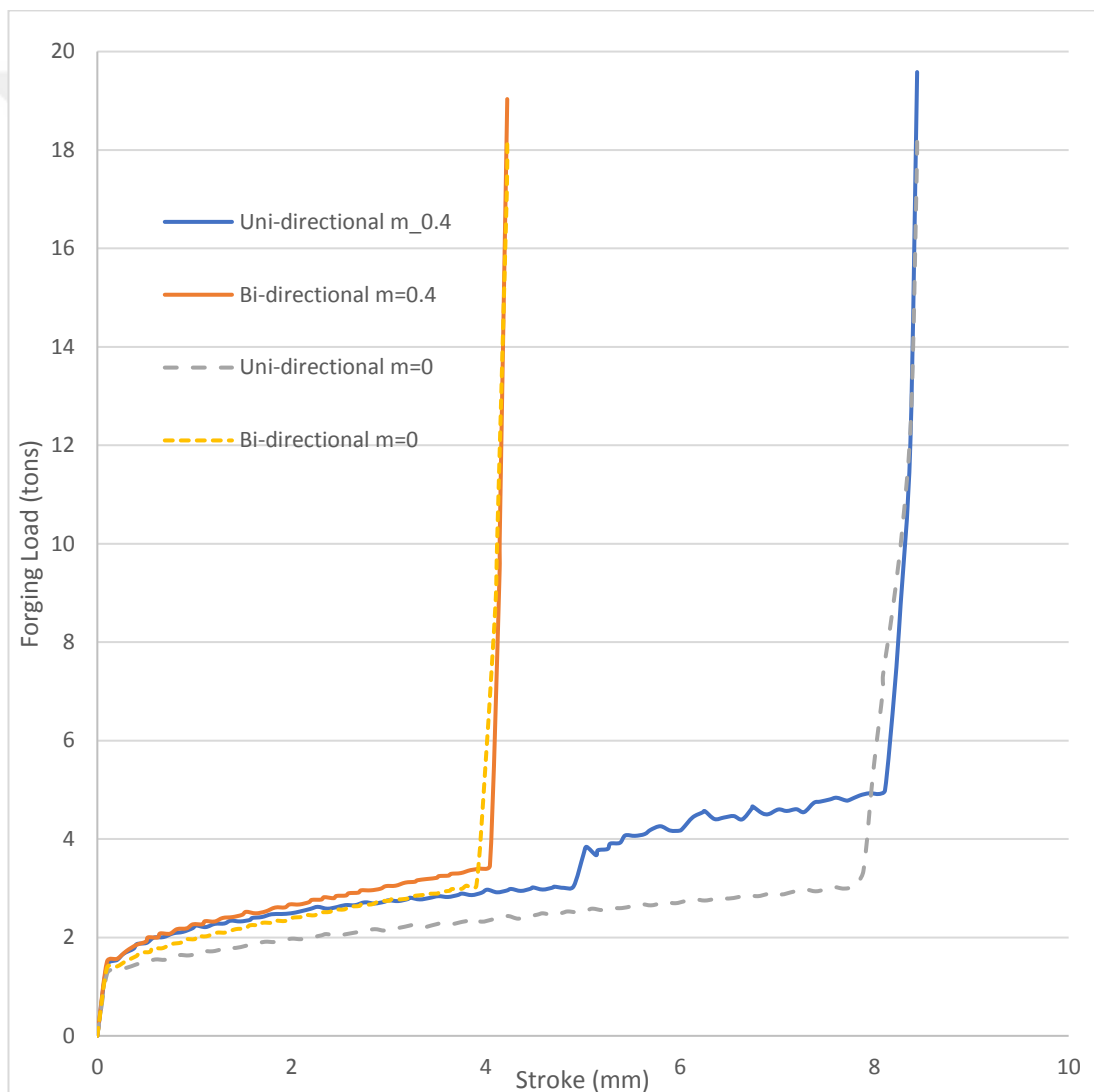
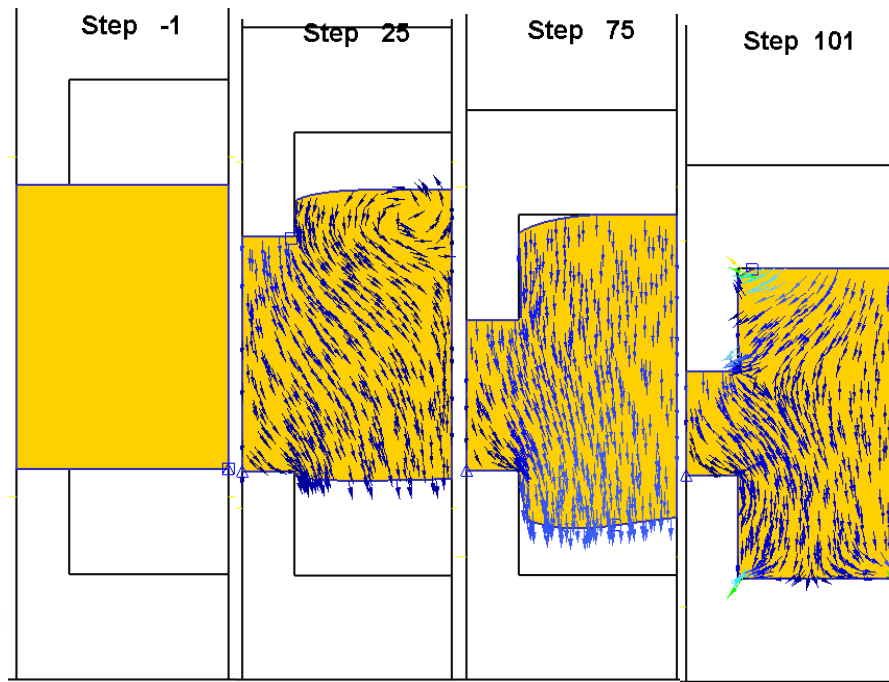
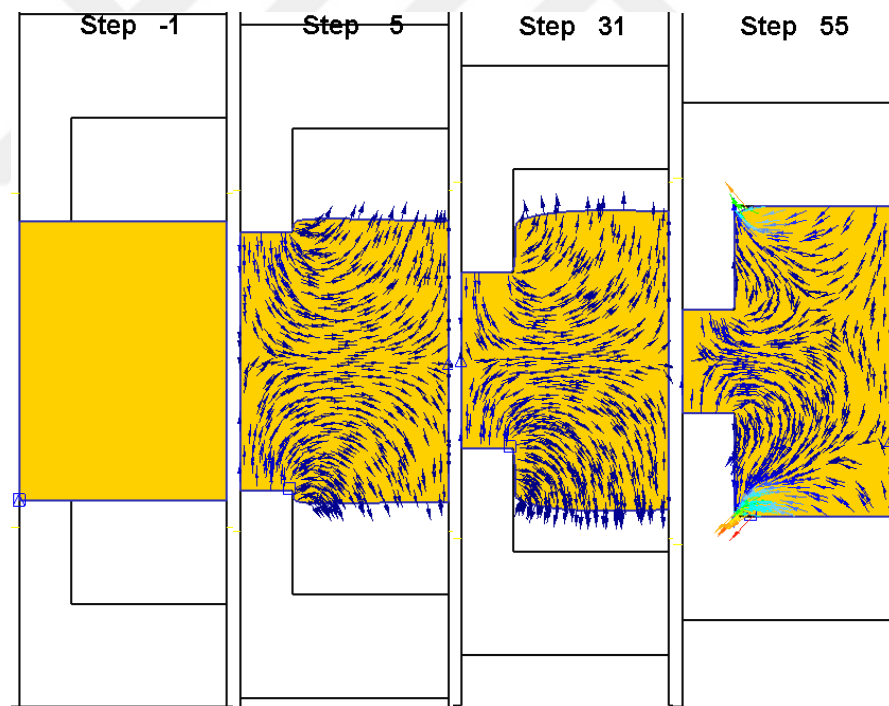


Figure 5.11 Uni-directional and Bi-directional forging loads with different friction factors for H1P2-shape ($m=0$ and $m=0.4$).



(a) Uni-directional loading



(b) Bi-directional loading.

Figure 5.12 Extrusion mode of the material flow pattern of H1-P2 -shape Aluminum 1100 with friction factor ($m=0.4$) forgings for a) uni-directional and b) bi-directional loading.

5.2.2.3 Dividing Metal Flow By Using Bi-Directional Step Forging Load

The results of uni-directional and bi-directional forgings show that the forging load asymptotically increases at the final filling stage. The material flow patterns show that at the final filling stage, whole body of the billet is forced to move. This cause deformation resistance (hydrostatic pressure encountered) and frictional resistance. At this stage, although vey small amount of material is displaced to fill the cavity, very high load is required. In order to reduce the forging load and to obtain complete die filling, bi-directional step forgings (divided-flow method) were performed on P1 and P2 preforms. The die set has got two upper and two lower punches as shown in Figure 5.13.

The movement of die components in each step is shown in Figure 5.14 and 5.15 for the bi-directional step loading of H1P1 and H1P2 forgings. In H1P1(Figure 5.14) forging, upper and lower punches are moved the first to reach the final height of the forging then the upper and lower rings are moved to complete the forging operation.

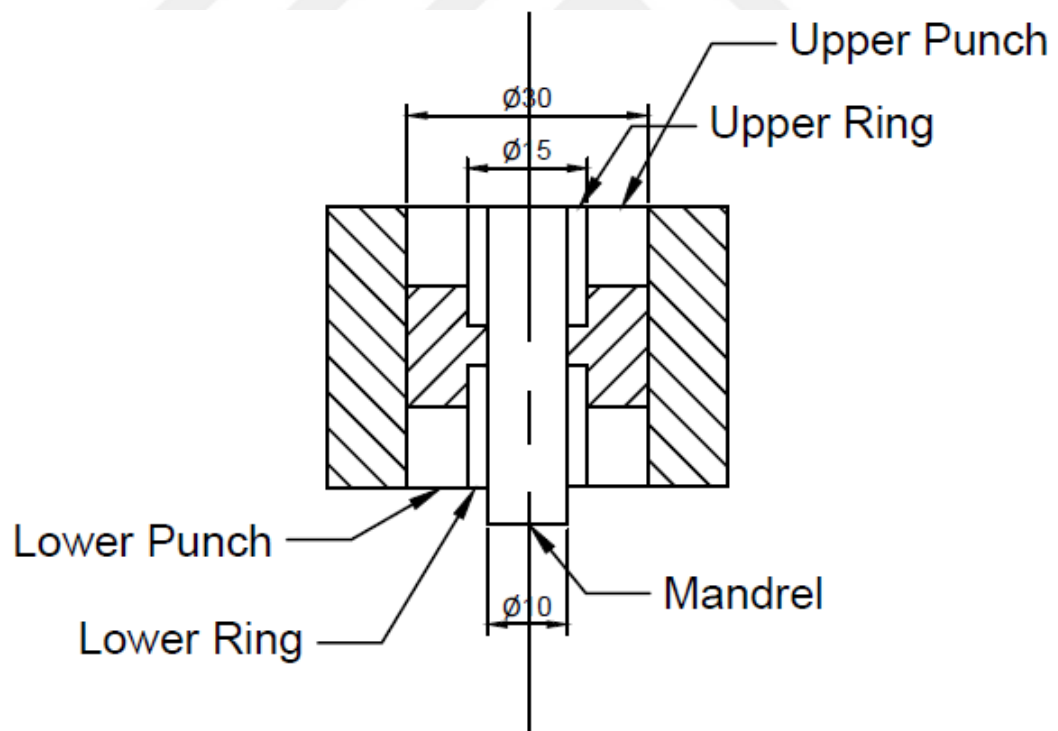


Figure 5.13 Sketch of Divided Flow Die Set for bi-directional step loading

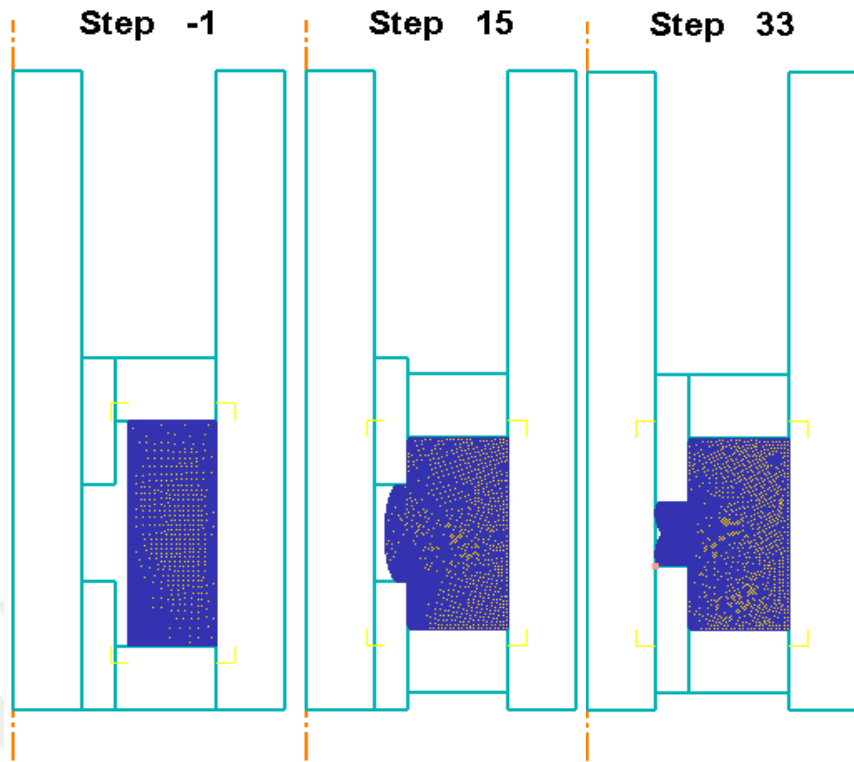


Figure 5.14 The FE output of H1P1-shape forgings Bi-directional step loading.

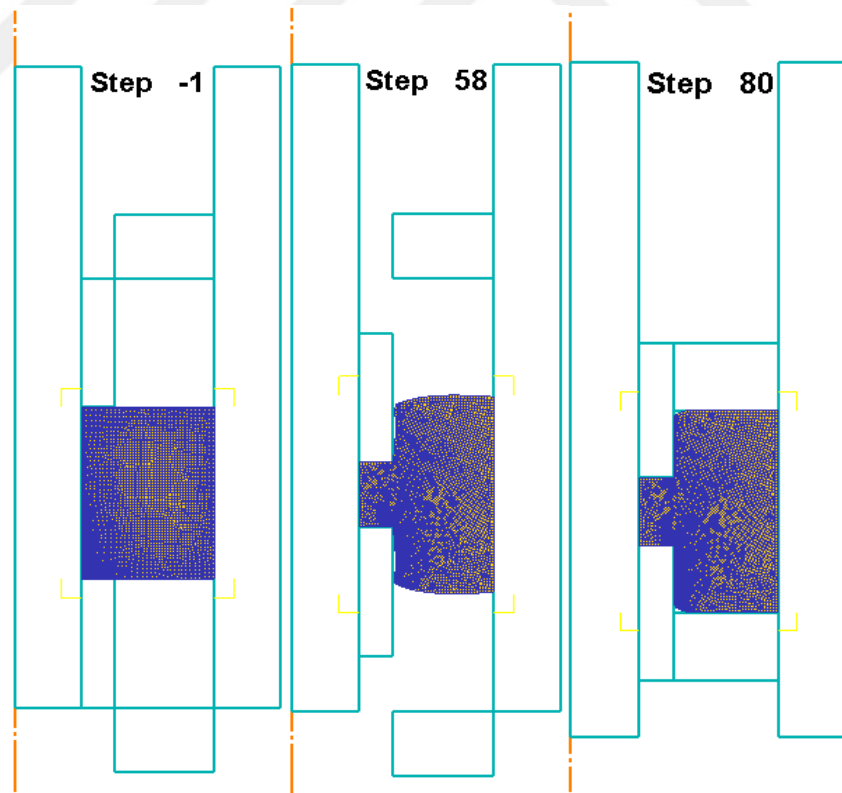


Figure 5.15 The FE output of H1P2-shape forgings Bi-directional step loading.

The load stroke diagrams of all loading conditions are shown in Figure 5.16 for friction factor $m=0.4$. The maximum loads are summarized in Table 5.4. The maximum loads on the upper punch in step 1 and on the upper ring in step 2 are 10.9 and 3.2 tons, respectively. The maximum load for complete filling is considerably reduced by step loading. In H1P2 (Figure 5.15) forging, upper and lower rings are moved first to reach the final hub height of the forging. Then the upper and lower punches are moved to complete the forging operation. The maximum loads for step 1 and step 2 are 3.4 and 14.3 tons, respectively. Similarly, the maximum load for complete filling is reduced by step loading for preform P2.

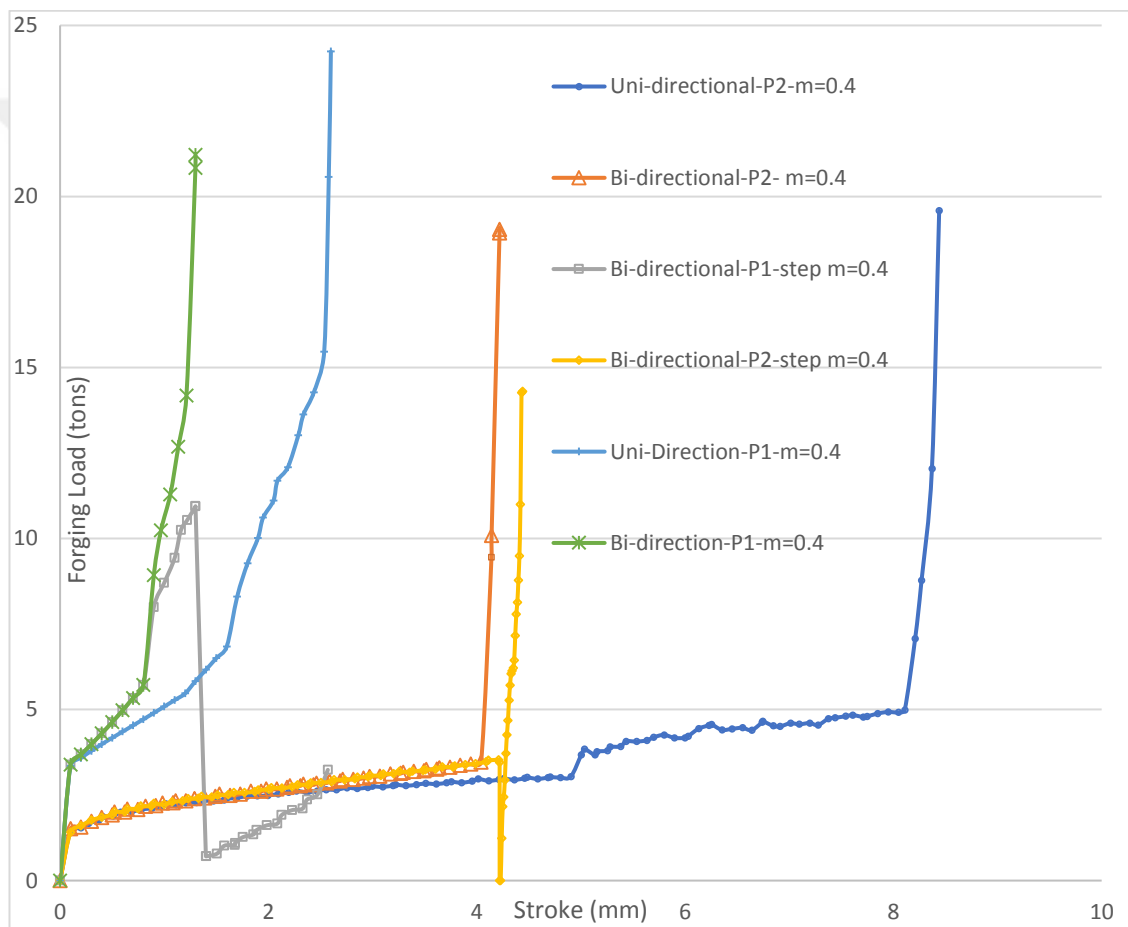


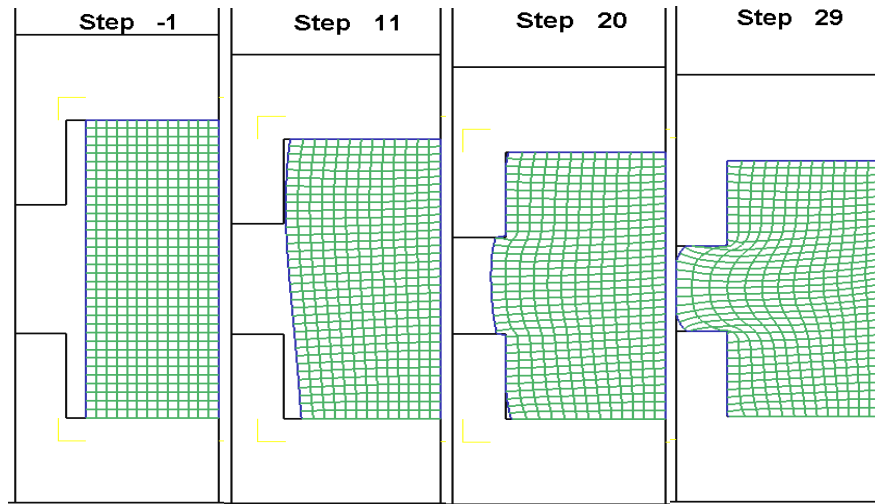
Figure 5.16 Uni-directional, bi-directional and bi-directional Step forging loads for H1P1 and H1P2 ($m=0.4$).

Table 5.4 The maximum loads for uni-directional, bi-directional and bi-directional step

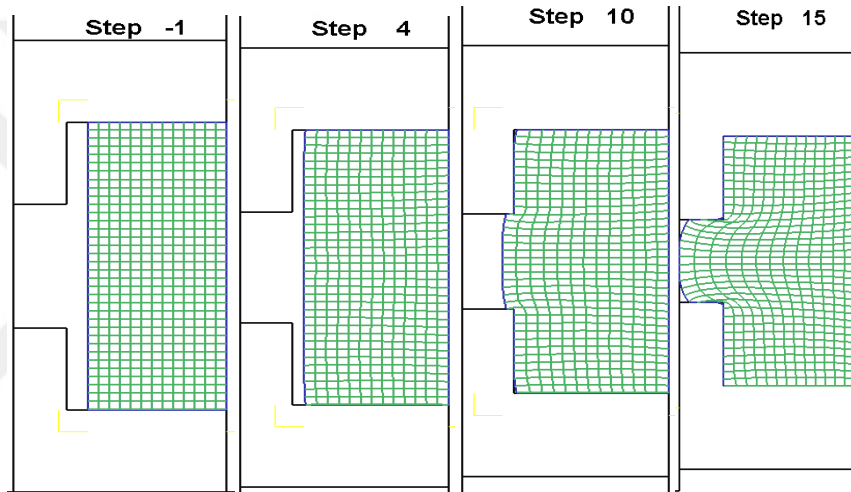
Part- Preform	Al 1100 Simulation Max Load (Tons) for H1P1, H1P2			
	Uni- Directional	Bi- Directional	Bi-Directional Step	
			Step1	Step2
H1P1	24.2	21.2	10.9	3.2
H1P2	19.6	19	3.4	14.3

5.2.2.4 Quality of forged product in terms of metal flow

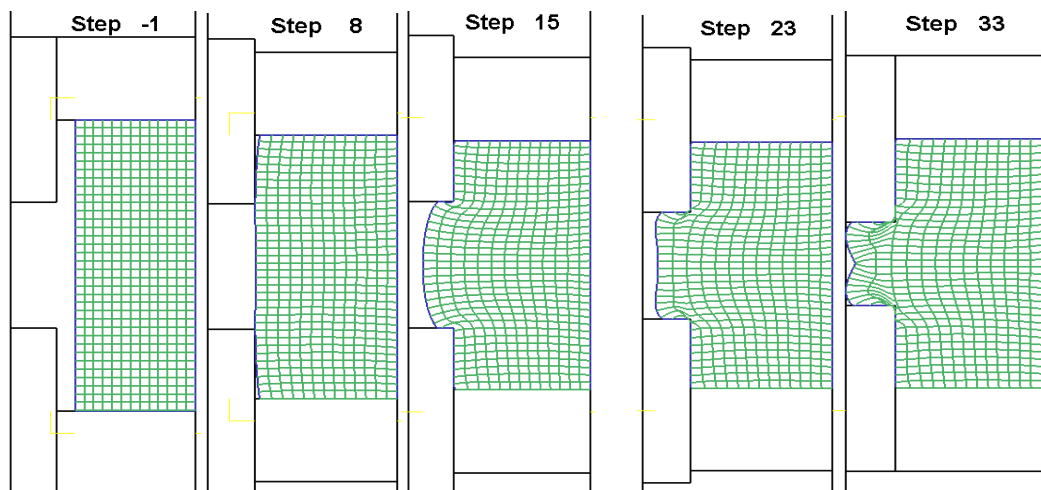
The advantage of forging over casting or machining is mainly due to grain flow (flow lines) orientation. This is depending on the material flow in the die cavity. The outmost objective is that the workpiece must completely fill the cavity without defects of material flow, such as pinching, shearing or folding. The orientation of flowlines of H-shape forgings for all loading conditions were obtained from DEFORM Flownet and are shown Figures 5.17 and 5.18. As observed from the figures, forgings using preform P2 have folding defects for all loading conditions and the uni-directional loading one is the worst. Determination of the folding defect is not easy on the forged product, because the folded surfaces weld to each other at high stresses and high temperature generated by friction on those surfaces. The weldment is weak and micro-cracks initiated easily under cyclic loading. Preform P1 (upset mode of deformation) is better for H-shape forgings in terms of flow line orientation.



(a) Uni-Directional

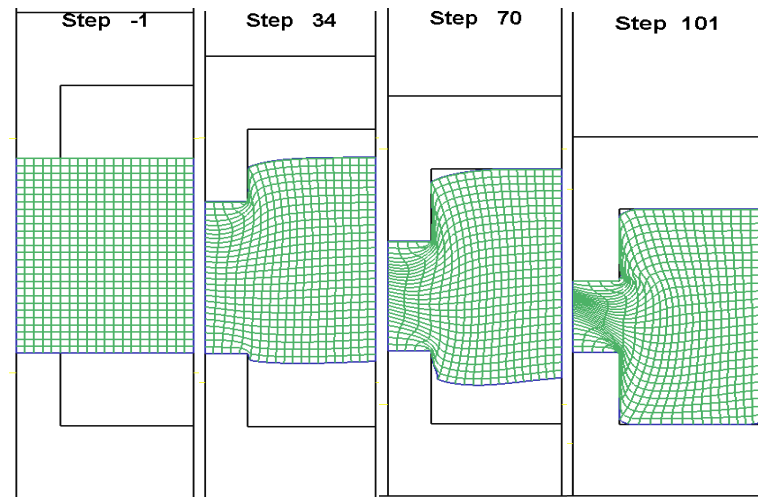


(b) Bi-Directional

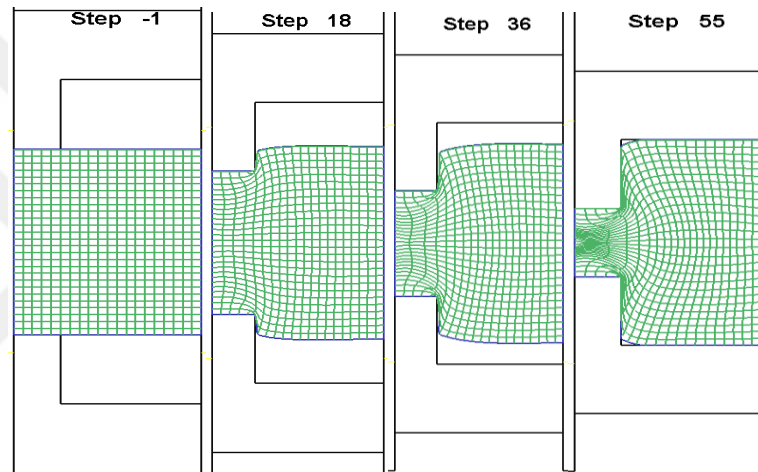


(c) Bi-Directional step

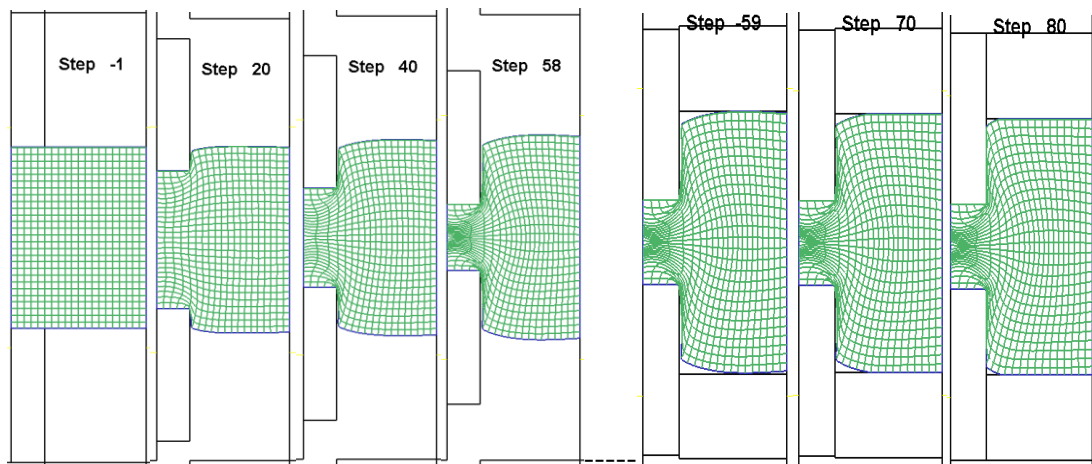
Figure 5.17 Flownet of H1P1-shape ($m=0.4$) for a) Uni-Directional b) Bi-Directional c) Bi-directional step



(a) Uni-Directional



(b) Bi-Directional



(c) Bi-Directional step

Figure 5.18 Flownet of H1P2-shape ($m=0.4$) for a)Uni-Directional b)Bi-Directional c) Bi-directional step

5.2.2.5 Effect of Rib Angle (α) on the Forging Load

In H-shape forgings, a rib angle (α) is generally added to increase the strength of the forged product and to eject the workpiece from the die easily. It is also preferred due to better material flow pattern (reducing shearing and folding). The effect of rib angle (α) on the forging load is shown in Figure 5.19. As seen from the figure, the addition of rib angle (α) has almost no effect on the maximum forging load. The slight change in maximum forging load with respect to rib angle is due to volume change during re-meshing in finite element analyses. Very small differences in final filling affecting maximum load which is asymptotic at this stage. The effects of rib angle on flow patterns are given in Figures 5.20 and 5.21. The folding at the hub corner is reduced especially for preform P2 in uni-directional loading condition. The velocity distribution of bi-directional forgings for H4P1 and H4P2 is also given in Figure 5.22.

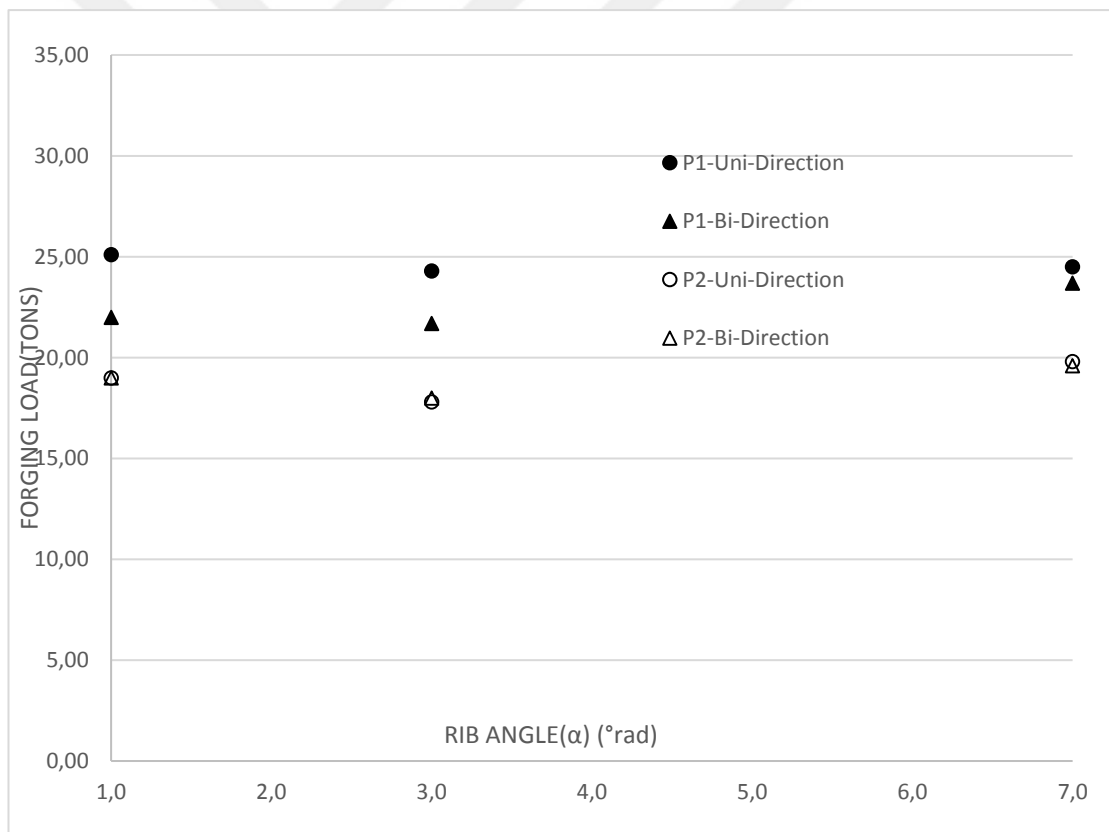
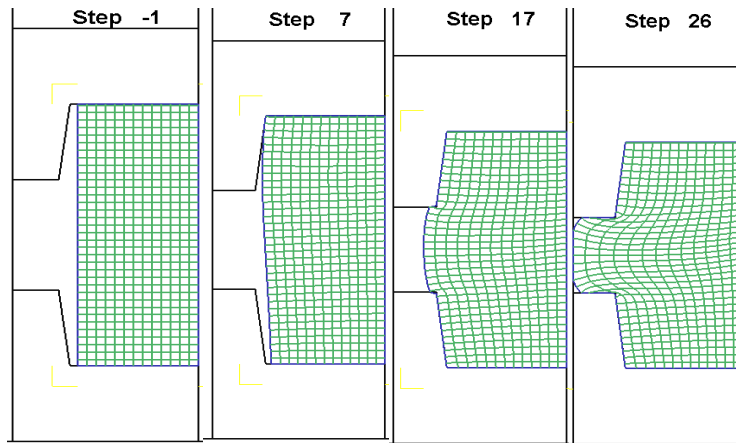


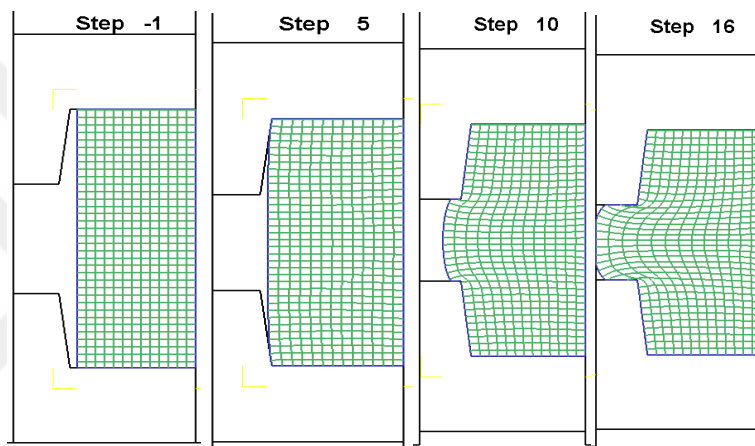
Figure 5.19 Effect of Rib Angle on the Forging Load

Table 5.5 The maximum forging loads for uni-directional, bi-directional and bi-directional step

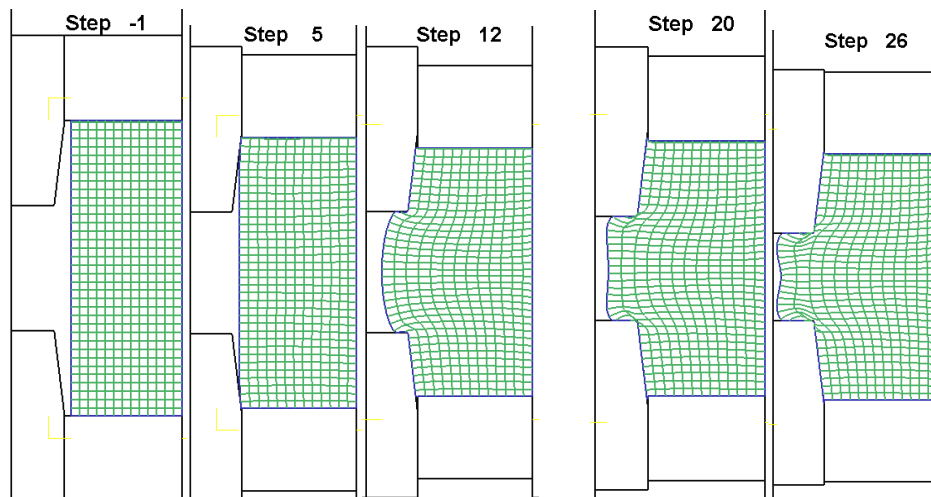
Part-Preform	Effect Of Rib Angle (α)(°rad) of Al 1100 Simulation Max Load (Tons)			
	Uni-Directional	Bi-Directional	Bi-Directional Step	
			Step1	Step2
H1P1 ($\alpha=0^\circ$)	24.2	21.2	10.9	3.2
H1P2 ($\alpha=0^\circ$)	19.6	19	3.4	14.3
H4P1 ($\alpha=7^\circ$)	24.5	23.7	10.4	3.1
H4P2 ($\alpha=7^\circ$)	19.6	19	3.3	13.9
H6P2($\alpha=22^\circ$)	21	19.5	3.2	12.1
H8P2($\alpha=45^\circ$)	22.8	20.5	3.1	11.5



(a) Uni-directional

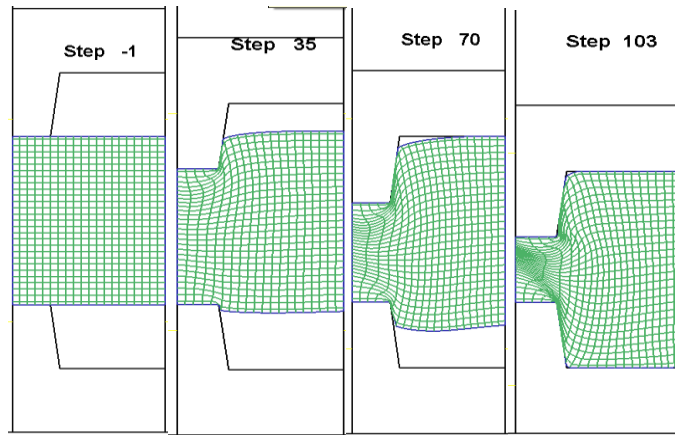


(b) Bi-directional

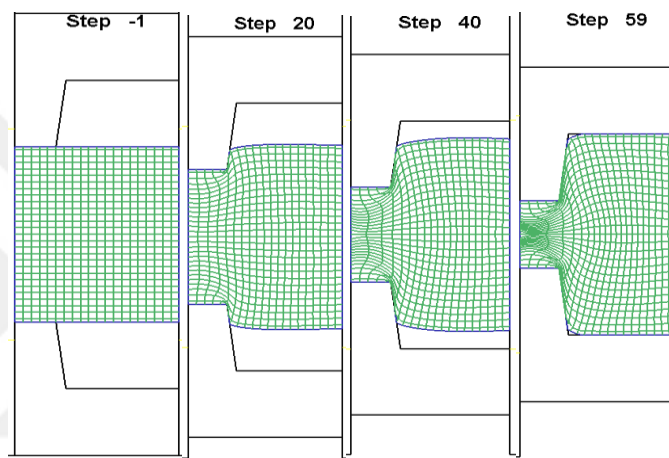


(c) Bi-directional step

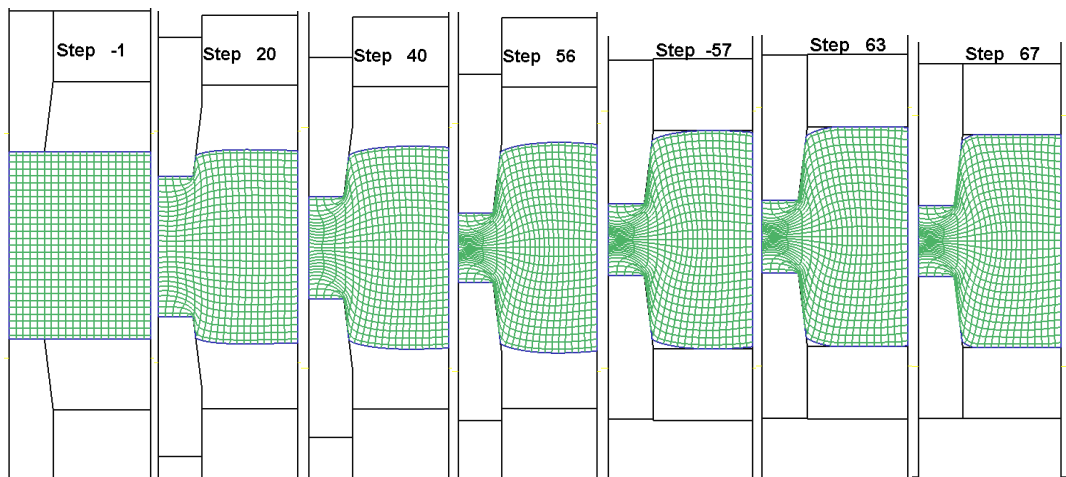
Figure 5.20 Flow net of H4P1 ($m=0.4$) for a)uni-directional b)bi-directional c) bi-directional step



(a) Uni-directional

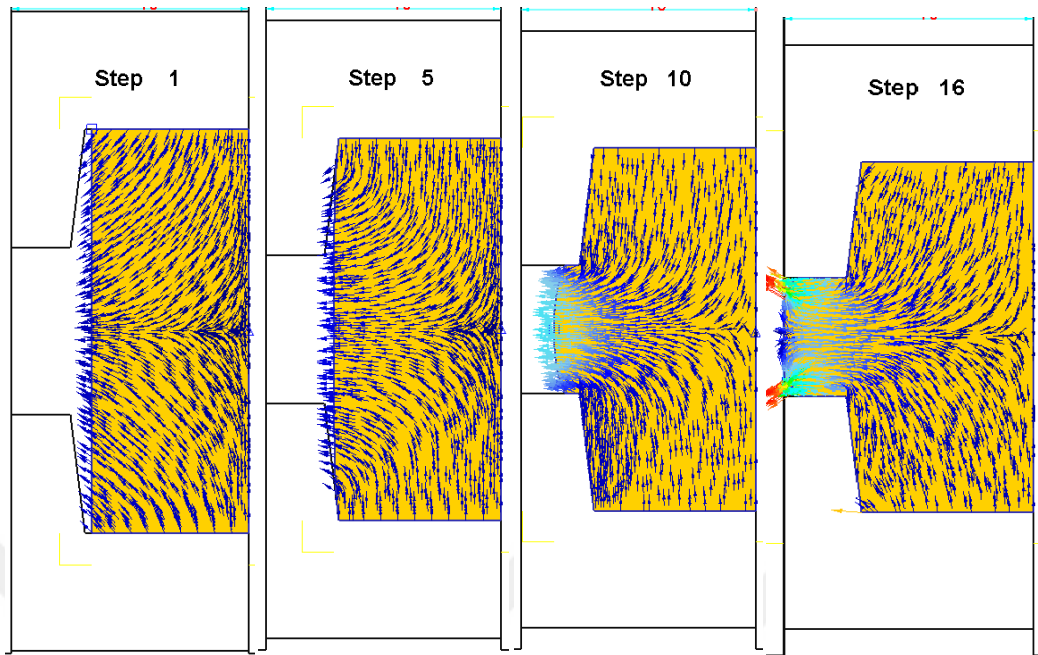


(b) Bi-directional

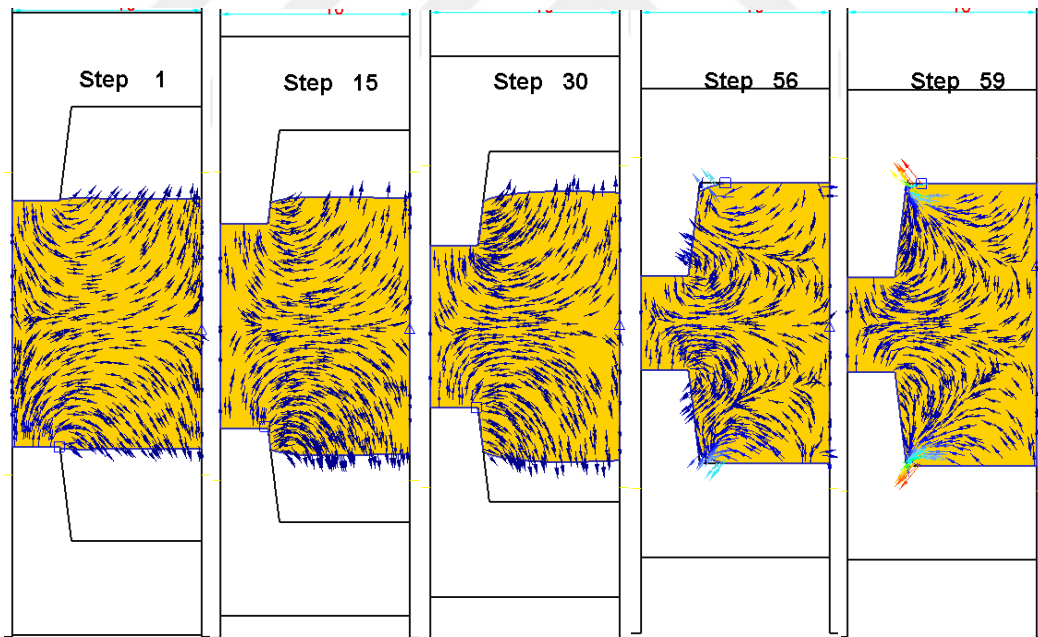


(c) Bi-directional step

Figure 5.21 Flownet of H4P2($m=0.4$) for a) uni-directional b) bi-directional c) bi-directional step



(a) H4P1 upset mode



(b) H4P2 extrusion mode

Figure 5.22 The velocity distribution of bi-directional forgings with friction factor ($m=0.4$) for a) H4P1 upset mode b) H4P2 extrusion mode

5.2.2.6 Effect of the Hub Thickness (t) on The Forging Load and Energy

The effect of hub thickness on the maximum forging load is shown in Figure 5.23. The maximum forging load is almost similar for different hub thicknesses of the same preform and loading condition. The small difference is due to the nature of finite element analyses (volume change during remeshing). Although the outer diameter and final height of the workpiece is constant, the initial height is changing with the hub thickness. The increase in preform height, increasing stroke length (punch movement) for preform P1 and reducing the stroke length for preform P2, so that the forging energies are increasing and decreasing for P1 and P2, respectively, as shown in Figure 5.24. Therefore, if the capacity of the press is enough, it is better to use preform P2 (extrusion mode) in terms of energy saving. (seen in Figure 5.24)

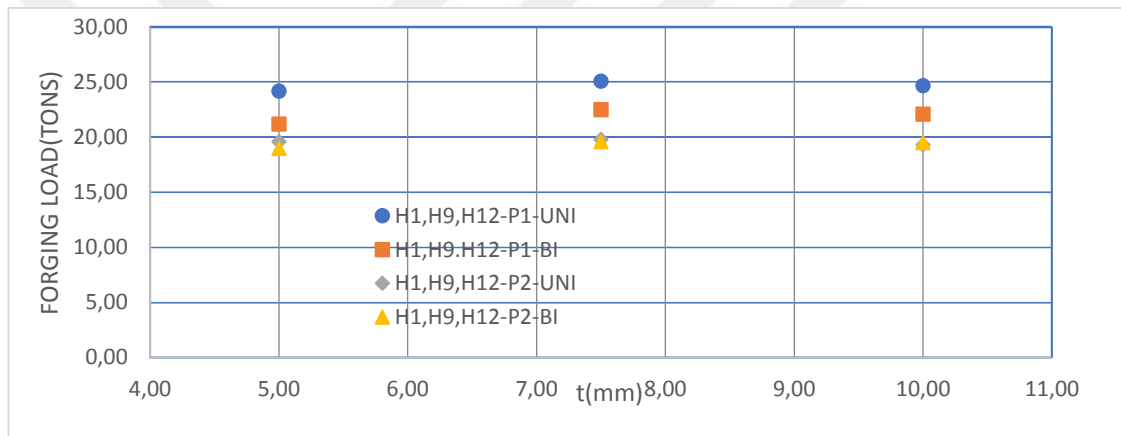


Figure 5.23 Uni-Directional and Bi-Directional Forging Loads according to hub thickness (t) for Preform P1 and P2 for H1, H9 and H12 parts

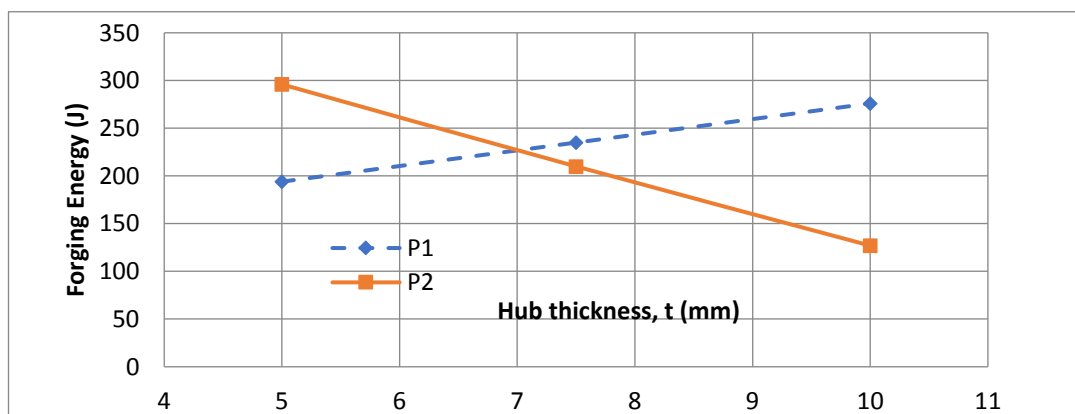


Figure 5.24 The change in forging energies with respect to hub thickness.

CHAPTER 6

CONCLUSION AND FUTURE WORK

6.1. Conclusions

From the experimental studies and FE simulations, the followings can be concluded:

1. The finite element model is verified by using the plasticine. So that the plasticine can be used as a physical modeling material for forging.
2. The forging load for uni-directional and bi-directional loading cases are increased with friction.
3. The results of uni-directional and bi-directional forgings show that the forging load asymptotically increases at the final filling stage. The material flow patterns show that at the final filling stage, whole body of the billet is forced to move. This cause deformation resistance and frictional resistance.
4. The use of bi-directional loading (enclosed die forging) in H-shape forging reduces maximum forging load and energy, thus, encounter lower die stresses.
5. The material flow in bi-directional forging of the H-shape is symmetrical while the flow in uni-directional forging is non-symmetrical. The non-uniform material flow increasing the deformation resistance and friction load. It may also causes folding defects on the final product.
6. Comparing to preform P1, preform P2 requires lower forging load but higher energy due to longer stroke to fill the die cavity. Extrusion mode of deformation (where material flow and punch movement are parallel to each other) is easier than upset mode of deformation (where material flow and punch movement are perpendicular to each other).

7. The maximum forging load is considerably reduced by using the bi-directional step loading (divided flow). The bi-directional step loading requires four movable components (punches) in the assembly, therefore, the usage of servo-driven presses are very effective.

8. The addition of rib angle (α) has almost no effect on the maximum forging load, but the folding at the hub corner is reduced especially for preform P2 in uni-directional loading condition.

9. The maximum forging load is almost similar for different hub thicknesses of the same preform and loading condition. Although the outer diameter and final height of the workpiece is constant, the initial height of the preform is changing with the hub thickness. The increase in preform height, increasing stroke length (punch movement) for preform P1 and reducing the stroke length for preform P2, so that the forging energies are increasing and decreasing for P1 and P2, respectively. Therefore, if the capacity of the press is enough, it is better to use preform P2 (extrusion mode) in terms of energy saving.

6.2. Future Work

The following areas may require further investigation about this study:

1. The experimental study can be performed on the aluminum and steel preforms by using a higher capacity servo press.
2. The forgings can be carried out by using different velocity profiles for each punch to control the metal flow.
3. The study may be extended for other axisymmetric shapes and non-symmetric parts.
4. The advantages of step loading may be further investigated for different forging especially for parts requiring very high forging loads.

REFERENCES

- [1] Shinozaki, K. (1992). Manufacturing of precision products by enclosed die forging, *JSTP (The Japan Society for Technology of Plasticity)*, **33**, 382.
- [2] Ohga, K., Kondo, K. (1993). Research on application range of the precision cold die forging utilizing divided flow to thick products, *Proc. 4th ICTP(International Centre for Theoretical Physics)*, p. 1239.
- [3] Yoshimura, H., Tanaka, K. (2000). Precision Forging of Aluminum and Steel, *J. Mater. Process. Technol.* **98**, 196–304.
- [4] Maccormack, C., Monaghan, J. (2002). 2D and 3D finite element analysis of a three-stage forging sequence, *Journal of Materials Processing Technology*, **127**, 48–56.
- [5] Osakada, K. (2010). Application of Servo Presses to Metal Forming Processes, *Steel Research Int.*, **81**, 9-16.
- [6] Nakano, T. (2010). Press Machine Trends and Servo Press Forming Examples, *Steel Research Int.*, **81**, 682-685.
- [7] Kawamoto, K., Klumb, D. (2012). Future Application of AC Servo Press Focusing on Forging Process, *Proceedings of the 45th ICFG (International Cold Forging Group) Plenary Meeting*, 113-116.
- [8] Osakada, K., Mori, K., Altan, T., Groche, P. (2011). Mechanical Servo Press Technology for Metal Forming, *CIRP Annals – Manufacturing Technology*, **60**, 651-672.
- [9] Yoshimura, H., Tanaka, K. (2000). Precision forging of aluminum and steel, *Journal of Materials Processing Technology*, **98**, 196-204.
- [10] Osakada, K., Wang, X., Hanami, S. (1997). Precision forging process with axially driven container, *Journal of Materials Processing Technology*, **71**, 105–112.

- [11] Shi, K., Shan, D.B., Xu, W.C., Lu, Y. (2007). Near net shape forming process of a titanium alloy impeller, *Journal of Materials Processing Technology*, **187-188**, 582–585.
- [12] Shan, D., Liu, F., Xu, W., Lu, Y., (2005). Experimental study on process of precision forging of an aluminum-alloy rotor, *Journal of Materials Processing Technology*, **170**, 412–415.
- [13] Gronostajski, Z., Hawryluk, M. (2008). The main Aspect of precision forging, *Archives of civil Mechanical Engineering*, **Vol.VIII No.2**, 39-55.
- [14] Behrens, A., Doege, E., Reinsch, S., Telkamp, K., Daehndel, H., Specker, A. (2007). Precision forging processes for high-duty automotive components, *Journal of Materials Processing Technology*, **185**, 139–146.
- [15] Shan, D.B., Wang, Z., Lu, Y., Xue, K.M. (1997). Study on isothermal precision forging technology for a cylindrical aluminum-alloy housing, *Journal of Materials Processing Technology*, **72**, 403–406.
- [16] Shan, D.B., Xu, W.C., Lu, Y. (2004). Study on precision forging technology for a complex-shaped light alloy forging, *Journal of Materials Processing Technology*, **151**, 289–293.
- [17] Cheng, W., Chi, C., Wang, Y., Lin, P., Zhao, R., Liang, W. (2015). 3D FEM simulation of flow velocity field for 5052 aluminum alloy multi-row sprocket in cold semi-precision forging process, *Trans. Nonferrous Met. Soc. China*, **25**, 926–935.
- [18] Guan, Y., Bai, X., Liu, M., Song, L., Zhao, G. (2014). 3D preform design in forging process based on quasi-quipotential field and response surface methods, *Procedia Engineering*, **81**, 468 – 473.
- [19] Kawamoto, K., Yoneyama, T., Okada, M., Kitayama, S., Chikahisa, J. (2014). Optimum back-pressure forging using servo die cushion, *Procedia Engineering*, **81**, 346-351.
- [20] Kim, S., Tsuruoka, K., Yamamoto, T. (2014). Effect of forming speed in precision forging process evaluated using CAE technology and high-performance servo-press machine, *Procedia Engineering*, **81**, 2451-2420.

- [21] Ngaile, G., Altan T., (2003). Computer Aided Engineering Forging, *ERC for Net Shape Manufacturing*, The Ohio State University,
- [22] MacCormack, C., Monaghan, J. (2002). 2D and 3D finite element analysis of a three-stage forging sequence, *Journal of Materials Processing Technology*, **127**, 48–56.
- [23] Petrov, P., Perfilov, V., Petrov, M., (2004). Development and research on near net shape forging technology of round part with flange made of aluminium alloy A95456, *10th International Conference of Metal Forming*, 1-8
- [24] Uğur, T., (2005). Evaluation of Metal Flow in Precision Forging of Axisymmetric Parts, *M. Sc.in Mechanical Engineering*, University of Gaziantep.
- [25] Zhang, Y., Shan, D., Xu, F., (2009). Flow lines control of disk structure with complex shape in isothermal precision forging, *Journal of materials processing technology*, **209**, 745–753.
- [26] Petrov, P., Perfilov, V., Stebunov, S. (2006). Prevention of lap formation in near net shape isothermal forging technology of part of irregular shape made of aluminium alloy A92618, *Journal of Materials Processing Technology*, **177**, 218–223.
- [27] Hartley, P., Pillinger, I. (2006). Numerical simulation of the forging process, *Comput. Methods Appl. Mech. Engrg.*, **195**, 6676–6690.
- [28] Park, K.S., Chester, J., Tyne, V., Moon, Y.H. (2007). Process analysis of multistage forging by using finite element method, *Journal of Materials Processing Technology*, **187–188**, 586–590.
- [29] Kopp, R. (1996). Some current development trends in metal forming technology, *J. Mater. Process. Technol.*, **60**, 1–10.
- [30] Heidelberg, S., Tekkaya, A.E. (2015). *60 Excellent Inventions in Metal Forming*.
- [31] Oudot, H., Faure, H. (April 2001). Improvement of Precision in Cold Forged Parts, *La Forge*, **No. 4**, p 27.

- [32] Altan, T., Ngaile, G., Shen, G., Cold and Hot Forging Fundamentals and Applications, *Editors*, p 319-335.
- [33] Shinozaki, K., Yoshimura, H., Ando, H., (1999), Enclosed die forging, Its prosperous aspect as a precision forging process, *40*, **459**, 316–321.
- [34] Kawamoto, K. (2014). Optimum back-pressure forging using servo die cushion, *Procedia Engineering*, **81**, 346-351.
- [35] Nakano, T., (March 31 to April 1, 1997). Presses for Cold Forging, *Aida Engineering Ltd., JSTP International Seminar of Precision Forging (Osaka, Japan), The Japanese Society for Technology of Plasticity*.
- [36] The Aida Digital Servo Former: NC-1 and NS-1, Hy-Flex D Series, *Aida Engineering Ltd.*
- [37] Valberg, S. (2010). Applied Metal Forming Including Fem Analysis, *Norwegian University of Science and Technology*, Cambridge University Press.
- [38] Kobayashi, S., Oh, S., Altan, T. (1989). Metal Forming and The Finite-Element Method, *New York Oxford, Oxford University Press*.
- [39] İsbir, S. S., (2002). Finite Element Analysis of Trimming, *M.S. Thesis, Middle East Technical University, Ankara*, p.24